

Fault-Resilient Continuum Deformation Coordination

Hossein Rastgoftar D, Member, IEEE

Abstract—This article offers a physics-based automation with two operation modes: 1) homogeneous deformation mode (HDM) and 2) containment exclusion mode (CEM), to safely plan a large-scale group coordination and resiliently recover safety in the presence of unpredicted agent failures. HDM becomes active when all agents are healthy, where the group coordination is defined by homogeneous transformation coordination functions. At HDM, a desired n-D homogeneous transformation (n=2,3) is uniquely related to the desired trajectories of n+1 leaders and acquired by the remaining followers in real-time through local communication. At CEM, agent coordination is treated as an ideal fluid flow, where the desired agents' paths are defined along stream lines inspired by fluid flow field theory to circumvent exclusion spaces surrounding failed agent(s). This article formally specifies the transitions between the HDM and CEM by using local proximity and applying the continuum deformation properties. More specifically, local proximity is used by agents to define interagent communication in an unsupervised fashion once they recover safety and HDM is activated. On the other hand, properties of homogeneous transformation are applied to quickly detect each arising anomalous situation and exclude failed agent(s) from group coordination of healthy agents.

Index Terms—Continuum deformation, decentralized control, local communication, physics-based methods, resilient multiagent coordination.

I. INTRODUCTION

ONTROL of multiagent systems has been widely investigated over the past two decades. Formation and cooperative control can reduce the cost and improve the robustness and capability of reconfiguration in a cooperative mission. Therefore, researchers have been motivated to explore diverse applications for the multiagent coordination, such as formation control [1], traffic congestion control [2], distributed sensing [3], and cooperative surveillance [4].

A. Related Work

Centralized and decentralized cooperative control approaches have been previously proposed for multiagent coordination. The

Manuscript received July 3, 2020; accepted September 5, 2020. Date of publication September 30, 2020; date of current version February 26, 2021. This work was supported by the National Science Foundation under Award Nos. 1914581 and 1739525. Recommended by Associate Editor G. Russo.

The author is with the Department of Mechanical Engineering, Villanova University, Philadelphia, PA 19085 USA (e-mail: hosseinr@umich.edu).

Digital Object Identifier 10.1109/TCNS.2020.3028021

virtual structure [5], [6] model treats agents as particles of a rigid body. Assuming that the virtual body has an arbitrary translation and rigid body rotation in a 3-D motion space, the desired trajectory of every agent is determined in a centralized fashion. Consensus [7]–[12] and containment control are the most common decentralized coordination approaches. Multiagent coordination using first-order consensus [13] and second-order consensus [7] has been extensively investigated by researchers in the past. Leader-based and leaderless consensus have been studied in [8], [9]. Stability of the retarded consensus method was studied in [14] and [15]. Finite-time multiagent consensus of continuous time systems is studied in [10] and [11]. Su *et al.* [12] evaluate consensus under a switching communication topology in the presence of disturbances.

More recently, researchers have investigated the resilient consensus problem and provided guaranteed conditions for reaching consensus in the presence of malicious agents [16]–[19]. Weighted mean subsequence reduced (W-MSR) is commonly used to detect an adversary and remove malicious agent(s) from the communication network of normal agents [18], [19]. r-robustness and (r,s)-robustness conditions are used to prove network resilience under consensus. Particularly, (f+1,f+1)-robustness is considered as the necessary and sufficient condition for resilience of the consensus protocol in the presence of f malicious agents [18].

Containment control is a decentralized leader-follower approach in which multiagent coordination is guided by a finite number of leaders and acquired by followers through local communication. Necessary and sufficient conditions for the stability of continuum deformation coordination have been provided in [20]. Ji et al. [21] study the convergence of containment control and demonstrate that followers ultimately converge to the convex hull defined by leaders. Containment control under fixed and switching communication protocols is studied in [22] and [23], respectively. The authors in [24] and [25] study finite-time containment stability and convergence. Containment control stability in the presence of communication delay is studied in [26] and [27]. Also, the authors in [28] and [29] offer a leader–follower affine transformation method for multiagent coordination where graph rigidity is explained to specify followers' communication weights based on agents' reference configuration.

Continuum deformation for large-scale coordination of multiagent systems is developed in [30]. Similar to containment control, continuum deformation is a leader–follower approach in which a group coordination is guided by a finite number of

2325-5870 © 2020 IEEE. Personal use is permitted, but republication/redistribution requires IEEE permission. See https://www.ieee.org/publications/rights/index.html for more information.

leaders and acquired by followers through local communication [31]. In a continuum deformation coordination, follower communication weights are consistent with leader agents' reference positions in the continuum deformation coordination. The continuum deformation method advances containment control by formal characterization of safety in large-scale coordination. Assuming, continuum deformation is given by a homogeneous transformation, interagent collision avoidance and agent follower containment are guaranteed in a continuum deformation coordination by assigning a lower limit on the eigenvalues of the Jacobian matrix of the homogeneous transformation. Therefore, a large number of agents participating in a continuum deformation coordination can safely and aggressively deform to pass through narrow passages in a cluttered environment.

B. Contributions and Outline

This article proposes a physics-inspired approach to the resilient multiagent coordination problem. In particular, multiagent coordination is modeled by an automation with two physics-based coordination modes: homogeneous deformation mode (HDM) and containment exclusion mode (CEM). HDM is active when all agents are healthy and can reach the desired coordination defined by a homogeneous deformation. In the HDM, agents are treated as particles of an n-D deformable body and the desired coordination, defined based on the trajectories of n+1 leaders forming an n-D simplex at any time t, is acquired by the followers through local communication. CEM is activated once an adversarial situation is detected due to unpredicted vehicle or agent failure. In CEM, the desired coordination is treated as an irrotational fluid flow, and adversarial agents are excluded from the safe planning space by combining ideal fluid flow patterns in a computationally efficient manner.

Compared to the existing literature and the author's previous work, this article offers the following contributions.

- 1) This article offers a novel physics-inspired approach for detection of anomalous situations in which unexpected vehicle failure(s) disrupt collective vehicle motion.
- 2) This article advances the existing continuum deformation coordination theory by relaxing the follower containment constraint and offering a tetrahedralization approach to assign followers' communication weights in an unsupervised fashion.
- 3) This article proposes a model-free guarantee condition for convergence and interagent collision avoidance in a large-scale homogeneous transformation.
- 4) This article proposes a tetrahedralization method to naturally establish/reestablish interagent communication links and weights, to classify agents as boundary and follower agents, and to determine leaders in an unsupervised fashion.
- 5) The author believe this is the first paper describing safe exclusion of a failed agent in a cooperative team with inspiration from fluid flow models.

This article is organized as follows. Preliminaries in Section II are followed by a resilient continuum deformation formulation in Section III. Physics-based models for the HDM and CEM are described in Sections IV and V, respectively. Operation of the resilient continuum deformation coordination is modeled by a

hybrid automation in Section VI. Simulation results presented in Section VII are followed by concluding remarks in Section VIII.

II. PRELIMINARIES

A. Position Notations

The following position notations are used throughout this article: $Actual\ position$ of agent i is denoted by $\mathbf{r}_i(t) = [x_i(t)y_i(t)z_i(t)]^T$ at time t. $Reference\ position$ of agent i, denoted by $\mathbf{r}_{i,0,\gamma} = [x_{i,0,\gamma}y_{i,0,\gamma}z_{i,0,\gamma}]^T$, is equal to the actual position of agent i when $\gamma \in \{\text{CEM}, \text{HDM}\}$ is started. Therefore, $\mathbf{r}_{i,0,\gamma}$ is constant for every agent i until γ is overridden.

Global desired position of agent i is defined by a continuum deformation function and denoted by $\mathbf{r}_{i,c,\gamma}(t) = [x_{i,c,\gamma}(t)y_{i,c,\gamma}(t)z_{i,c,\gamma}(t)]^T$ at time t where $\gamma \in \{\mathrm{HDM}, \mathrm{CEM}\}.$

Local desired position of agent i is denoted by $\mathbf{r}_{i,d,\gamma}(t) = [x_{i,d}(t)y_{i,d}(t)z_{i,d}(t)]^T$ and defined as follows:

$$\mathbf{r}_{i,d}(t) = \begin{cases} \mathbf{r}_{i,c,\gamma}(t) & \gamma = \text{CEM} \land i \in \mathcal{V} \\ \mathbf{r}_{i,c,\gamma}(t) & \gamma = \text{HDM} \land i \in \mathcal{V}_L \\ \sum_{\forall j} w_{i,j} \mathbf{r}_j(t) & \gamma = \text{HDM} \land i \in \mathcal{V}_F \end{cases}$$
(1)

at time t where $w_{i,j}$ is the communication weight between agent i and j. Note that agent i acquires the desired coordination by tracking the local desired trajectory $\mathbf{r}_{i,d}$, i.e., $\mathbf{r}_{i,d}$ is the reference input to the control system of agent i. If $\gamma = \mathrm{HDM}$, $\mathbf{r}_{i,d}$ is updated through local communication and defined based on actual positions of the in-neighbors of agent i. Otherwise, $\mathbf{r}_{i,d} = \mathbf{r}_{i,c,\mathrm{CEM}}$ is assigned in a centralized fashion.

B. Motion Space Tetrahedralization and Λ Operator

Let $\mathbf{c} \in \mathbb{R}^{3 \times 1}$ and $\mathbf{p}_1, \mathbf{p}_2, \ldots, \mathbf{p}_{n+1} \in \mathbb{R}^{3 \times 1}$ be n+2 arbitrary position vectors in a 3-D motion space. Then, rank operator \varkappa_n is defined as follows:

$$\varkappa_n(\mathbf{p}_1,\ldots,\mathbf{p}_n) = \operatorname{rank}\left(\begin{bmatrix}\mathbf{p}_2 - \mathbf{p}_1 & \cdots & \mathbf{p}_{n+1} - \mathbf{p}_1\end{bmatrix}\right).$$
(2

If $\mathbf{p}_1, \dots, \mathbf{p}_{n+1}$ are positioned at the vertices of an n-D simplex, then $\varkappa_n(\mathbf{p}_1, \dots, \mathbf{p}_n) = n$.

Remark 1: This article studies 2-D and 3-D homogeneous deformation coordination problems; therefore, n=2,3. $\mathbf{p_1}$, $\mathbf{p_2}$, $\mathbf{p_3}$, and $\mathbf{p_4}$ form a tetrahedron for n=3, if $\varkappa_3(\mathbf{p_1},\mathbf{p_2},\mathbf{p_3},\mathbf{p_4})=3$. $\mathbf{p_1}$, $\mathbf{p_2}$, and $\mathbf{p_3}$ form a triangle for n=2, if $\varkappa_2(\mathbf{p_1},\mathbf{p_2},\mathbf{p_3})=2$.

Vector function \mathbf{p}_4^n : $\mathbf{p}_1, \dots, \mathbf{p}_{n+1}$ denote positions of n+1 points in a 3-D motion space where $\varkappa_n(\mathbf{p}_1, \dots, \mathbf{p}_{n+1}) = n$ ($n \in \{2,3\}$). Then, $\mathbf{p}_1, \mathbf{p}_2, \mathbf{p}_3$, and \mathbf{p}_4^n define vertices of a tetrahedron in a 3-D motion space if \mathbf{p}_4^n is defined as follows:

$$\mathbf{p}_{4}^{n} = \begin{cases} \mathbf{p}_{1} + \Xi \left(\mathbf{p}_{3} - \mathbf{p}_{1}\right) \times \left(\mathbf{p}_{2} - \mathbf{p}_{1}\right) & n = 2\\ \mathbf{p}_{4} & n = 3 \end{cases}$$
(3)

where $\Xi \neq 0$ (See Fig. 1).

Vector function \mathbf{c}^n : Suppose $\mathbf{p}_1, \dots, \mathbf{p}_{n+1}$ and \mathbf{c} denote positions of n+2 points in a 3-D motion space, where $\varkappa_n(\mathbf{p}_1, \dots, \mathbf{p}_{n+1}) = n$ and $n \in \{2, 3\}$. Then, we can define

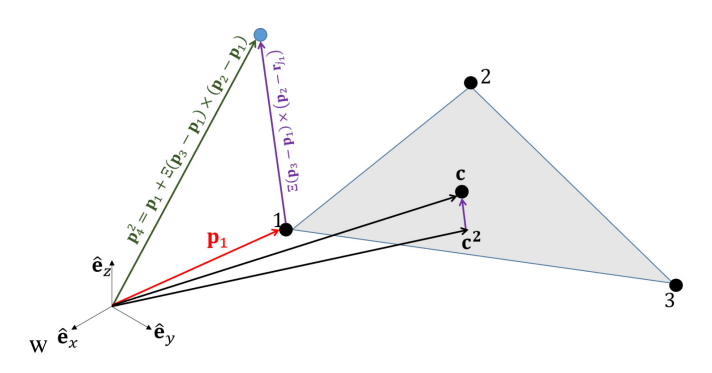


Fig. 1. Graphical representation of the virtual agent \mathbf{p}_4^2 .

vector function

$$\mathbf{c}^{n} = \begin{cases} \mathbf{c} - (\mathbf{c} \cdot \mathbf{n}_{1-4} (\mathbf{p}_{1}, \mathbf{p}_{2}, \mathbf{p}_{3})) \, \mathbf{n}_{1-4} (\mathbf{p}_{1}, \mathbf{p}_{2}, \mathbf{p}_{3}) & n = 2 \\ \mathbf{c} & n = 3 \end{cases}$$
(4)

where "." is the dot product symbol and unit vector

$$\mathbf{n}_{1-4}\left(\mathbf{p}_{1}, \mathbf{p}_{2}, \mathbf{p}_{3}\right) = \frac{\left(\mathbf{p}_{3} - \mathbf{p}_{1}\right) \times \left(\mathbf{p}_{2} - \mathbf{p}_{1}\right)}{\|\left(\mathbf{p}_{3} - \mathbf{p}_{1}\right) \times \left(\mathbf{p}_{2} - \mathbf{p}_{1}\right)\|}$$
 (5)

is normal to the triangular plane made by p_1 , p_2 , and p_3 .

Remark 2: Vector \mathbf{c}^2 is the projection of \mathbf{c} on the triangular plane made by \mathbf{p}_1 , \mathbf{p}_2 , and \mathbf{p}_3 (See Fig. 1).

Vector function Λ : Suppose \mathbf{p}_1 , \mathbf{p}_2 , \mathbf{p}_3 , and \mathbf{p}_4^n are known points in a 3-D motion space, where $\varkappa_3(\mathbf{p}_1, \mathbf{p}_2, \mathbf{p}_3, \mathbf{p}_4^n) = 3$ for $n \in \{2, 3\}$. Then, we can define a vector function

$$\mathbf{\Lambda}\left(\mathbf{p}_{1}, \mathbf{p}_{2}, \mathbf{p}_{3}, \mathbf{p}_{4}^{n}, \mathbf{c}^{n}\right) = \begin{bmatrix} \mathbf{p}_{1} & \mathbf{p}_{2} & \mathbf{p}_{3} & \mathbf{p}_{4}^{n} \\ 1 & 1 & 1 & 1 \end{bmatrix}^{-1} \begin{bmatrix} \mathbf{c}^{n} \\ 1 \end{bmatrix} \in \mathbb{R}^{4 \times 1}$$
(6)

that has the following properties [32]:

- 1) The sum of the entries of Λ is 1 for any configuration of vectors $\mathbf{p}_1, \dots, \mathbf{p}_4^n$ and \mathbf{c}^n for n = 2, 3.
- 2) If $\Lambda \geq 0$, \mathbf{c}^n is inside the tetrahedron formed by $\mathbf{p}_1, \ldots, \mathbf{p}_4^n$. Otherwise, it is outside the tetrahedron.

Proposition 1: If n=2, $\lambda_4(\mathbf{p}_1,\mathbf{p}_2,\mathbf{p}_3,\mathbf{p}_4^2,\mathbf{c}^2)=0$ for any arbitrary position \mathbf{c}^2 , where $\lambda_4(\mathbf{p}_1,\mathbf{p}_2,\mathbf{p}_3,\mathbf{p}_4^2,\mathbf{c}^2)$ is the fourth entry of vector. $\Lambda(\mathbf{p}_1,\mathbf{p}_2,\mathbf{p}_3,\mathbf{p}_4^2,\mathbf{c}^2)$.

Vector function Λ will be used in this article to determine boundary and interior agents, to specify followers' in-neighbor agents, to assign followers' communication weights in a 2-D and 3-D homogeneous deformation coordination, and to detect anomalies in a group coordination.

III. PROBLEM STATEMENT

Let $\Omega_{\mathrm{con}} \subset \mathbb{R}^3$ be a compact region in a 3-D motion space containing N(t) healthy and anomalous agents at time t, where dynamics of vehicle $i \in \mathcal{V}$ is given by

$$\dot{\mathbf{x}}_i = \mathbf{f}_i(\mathbf{x}_i, \mathbf{u}_i).$$

We say that $\mathbf{x}_i \in \mathbb{R}^{n_{\mathbf{x},i} \times 1}$ and $\mathbf{u}_i \in \mathbb{R}^{n_{\mathbf{u},i} \times 1}$ are the state and input vectors; actual position $\mathbf{r}_i = [x_i \ y_i \ z_i]^T$ of agent i is the

output of the control system of agent i. Set $\mathcal{V}(t)$ defines the identification (index) numbers of agents and expressed as follows:

$$\mathcal{V}(t) = \mathcal{V}_H(t) \left[\begin{array}{c} \mathcal{V}_A(t) \end{array} \right]$$
 (7)

where disjoint sets $\mathcal{V}_H(t)$ and $\mathcal{V}_A(t)$ define the index numbers of healthy and anomalous agents, respectively. Note that $N_H(t) = |\mathcal{V}_H(t)|$ is the total number of healthy agents, and $N(t) - N_H(t) = |\mathcal{V}_A(t)|$ is the total number of anomalous agents. Healthy agents reach the group desired coordination while *anomalous* agents do not.

In this article, the containment domain $\Omega_{\rm con}$ is rigid, where it does not deform or rotate at any time t. Therefore, $\Omega_{\rm con}$ can be expressed as $\Omega_{\rm con} = \Omega_{\rm con}({\bf r},{\bf r}_{\rm cont})$ where ${\bf r} \in \mathbb{R}^3$ denotes position and

$$\mathbf{r}_{\text{con}}(t) = \frac{1}{N_H(t)} \sum_{i \in \mathcal{V}_H(t)} \mathbf{r}_i(t)$$
 (8)

is the characteristic position of $\Omega_{\rm con}$ at time t. While anomalous agents are wrapped from the motion space by closed surfaces, healthy agents are treated as particles of a deformable body where the desired trajectory of agent $i \in \mathcal{V}_{\mathcal{H}}(t)$ is given by

$$\gamma \in \Gamma, \quad \dot{\mathbf{r}}_{i,c,\gamma} \left(\mathbf{r}_{i,c,\gamma}, t \right) = \mathbf{H}_{i,\gamma} \left(\mathbf{r}_{i,c,\gamma} \right) \dot{\mathbf{q}}_{\gamma}(t)$$
 (9)

set $\Gamma = \{\text{CEM}, \text{HDM}\}\$ specifies the collective motion operation modes. $\mathbf{r}_i = [x_{i,c,\gamma}(t) \ y_{i,c,\gamma}(t) \ z_{i,c,\gamma}(t)]^T$ is the global desired trajectory of agent $i \in \mathcal{V}_H(t)$, $\mathbf{q} = [q_{1,\gamma} \dots q_{m,\gamma}(t)]^T$ is the generalized coordinate vector, and $q_{1,\gamma}(t)$ through $q_{m,\gamma}(t)$ are the *generalized coordinates* specifying the temporal behavior of the group coordination. Furthermore,

$$i \in \mathcal{V}_H, \gamma \in \Gamma, \quad \mathbf{H}_{i,\gamma} = \begin{bmatrix} \mathbf{h}_{i,1,\gamma} & \cdots & \mathbf{h}_{i,m,\gamma} \end{bmatrix} \in \mathbb{R}^{3 \times m}$$
(10)

is the spatially varying *shape matrix* and $\mathbf{h}_{i,l,\gamma}(\mathbf{r}_{i,c,\gamma}) \in \mathbb{R}^{3 \times 1}$ is the l-th shape vector $(l \in \{1,\ldots,m\})$.

 $HDM(\gamma = HDM)$ is active when $\mathcal{V}_A(t) = \emptyset$ at time t. Therefore, $N_H(t) = N(t)$ agents defined by set \mathcal{V}_H are all healthy. The HDM shape matrix $\mathbf{H}_{i, \mathrm{HDM}}$ is constant everywhere in the motion space.

CEM ($\gamma=CEM$) is activated once at least one anomalous agent is detected in which case $\mathcal{V}_A \neq \emptyset$. At CEM, healthy agents are treated as particles of the ideal fluid flow; thus, the spatially varying shape matrix $\mathbf{H}_{i,CEM}$ determines the geometry of desired path of healthy agent $i \in \mathcal{V}_H$.

This article offers an automation with two operation modes HDM and CEM to resiliently recover a sudden failure in a large-scale continuum deformation coordination. In particular, we study the three main problems described below.

A. Problem 1: Physics-Based Modeling of HDM

For HDM, the collective motion is treated as particles of a deformable body, where the agent team desired coordination is defined by a homogeneous transformation. At HDM agents are classified as leaders and followers, where set \mathcal{V}_H is expressed as

$$\mathcal{V}_H(t) = \mathcal{V}_L(t) \bigcup \mathcal{V}_F(t).$$
 (11)

A desired n-D homogeneous deformation is guided by n+1 leaders defined by set \mathcal{V}_L . Leaders, defined by \mathcal{V}_L , move

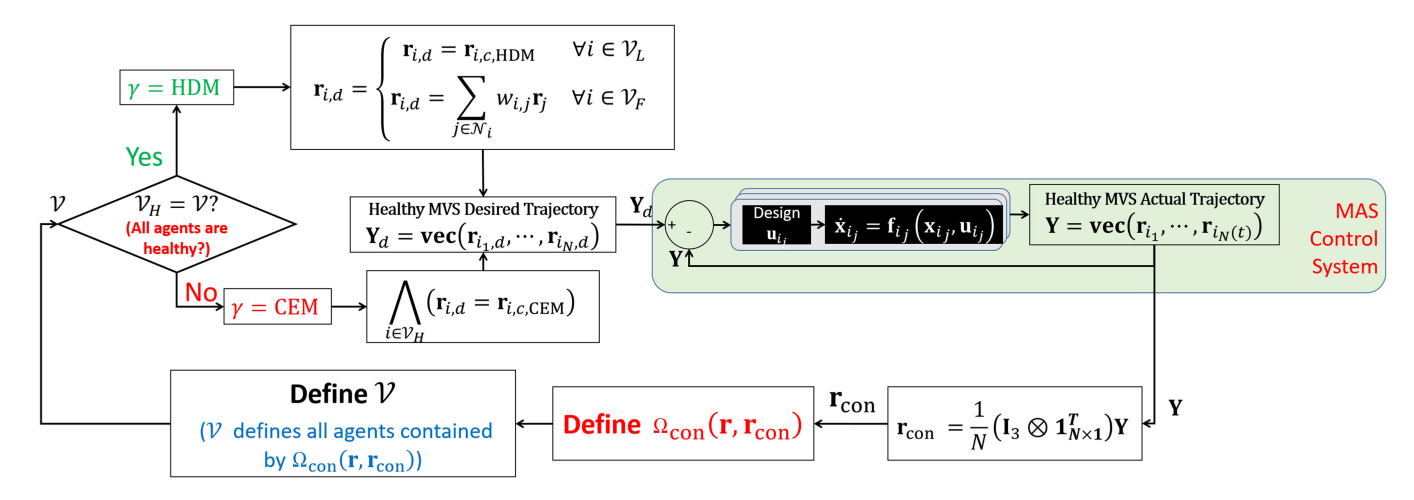


Fig. 2. Proposed automation for fault-resilient continuum deformation coordination.

independently and form an n-D simplex at any time t. Followers, defined by \mathcal{V}_F , acquire the desired coordination through local communication with their in-neighbor agents. This article offers a new tetrahedralization method to determine leaders and followers and to define interagent communication in an unsupervised fashion given an arbitrary reference configuration of agents.

B. Problem 2: Physics-Based Modeling of CEM

For CEM, it is desired that healthy agents move on surface z(x,y,t)= constant, where x and y components of the desired agent coordination are defined by an irrotational flow field. A potential function $\phi(x,y,t)$ and stream function $\psi(x,y,t)$ are defined so that the x-y plane is divided into safe region $\mathcal S$ and unsafe region $\mathcal U$ wrapping the anomalous agents. Note that both stream and potential functions satisfy Laplace equation: $\partial^2\phi/\partial x^2+\partial^2\phi/\partial y^2=0$ and $\partial^2\psi/\partial x^2+\partial^2\psi/\partial y^2=0$.

At CEM, every agent $i \in \mathcal{V}_H$ slides along the ith streamline defined by

$$\psi\left(x_{i,c,\text{CEM}}, y_{i,c,\text{CEM}}, t\right) = \psi_{i,0}(\text{constant}) \tag{12}$$

at any time $t \geq t_{\text{CEM}}$ and t_{CEM} is the start time of the CEM. Therefore, the desired trajectory of vehicle $i \in \mathcal{V}_H$ satisfies the following constraint at any time t:

$$\frac{\partial \psi(x_{i,c,\text{CEM}}, y_{i,c,\text{CEM}}, t)}{\partial x_{i,c,\text{CEM}}} \frac{dx_{i,c,\text{CEM}}}{dt} + \frac{\partial \psi(x_{i,c,\text{CEM}}, y_{i,c,\text{CEM}}, t)}{\partial y_{i,c,\text{CEM}}} \frac{dy_{i,c}}{dt} = 0.$$
(13)

Note that

$$\psi\left(x_{i,0,\text{CEM}}, y_{i,0,\text{CEM}}, t_{\text{CEM}}\right) = \psi_{i,0}$$

where $x_{i,0,\text{CEM}}$ and $y_{i,0,\text{CEM}}$ are the x and y components of reference position of agent $i \in \mathcal{V}_H$ at CEM.

Remark 3: A one-to-one mapping exists between $(x_{i,c,\text{CEM}}(t), y_{i,c,\text{CEM}}(t))$ and $(\phi_{i,c}(t), \psi_{i,c}(t))$ at any time t where $\phi_{i,c}(t) = \phi(x_{i,c,\text{CEM}}, y_{i,c,\text{CEM}}, t)$ and

 $\psi_{i,c}(t) = \psi(x_{i,c,\text{CEM}}, y_{i,c,\text{CEM}}, t)$. Thus, the Jacobian matrix

$$\mathbf{J}(x_{i,c,\text{CEM}}, y_{i,c,\text{CEM}}, t) = \begin{bmatrix} \frac{\partial \phi_{i,c}(t)}{\partial x_{i,c,\text{CEM}}} & \frac{\partial \phi_{i,c}(t)}{\partial y_{i,c,\text{CEM}}} \\ \frac{\partial \phi_{i,c}(t)}{\partial x_{i,c,\text{CEM}}} & \frac{\partial \phi_{i,c}(t)}{\partial y_{i,c,\text{CEM}}} \end{bmatrix}$$
(14)

is nonsingular at $(x_{i,c,CEM}, y_{i,c,CEM}) \in \mathcal{S}$ and $t \geq t_{CEM}$.

C. Problem 3: Continuum Deformation Anomaly Management

This article uses the properties of homogeneous deformation coordination to quickly identify failed agent(s) and formally specify the transition condition from HDM to CEM by comparing certain transient distance, computed at current time t, and reference communication weights assigned based on agents' reference positions. Also, transition from CEM to HDM is commanded once safety is recovered and all agents enclosed by $\Omega(\mathbf{r}, \mathbf{r}_{con})$ are healthy. The flowchart in Fig. 2 shows the functionality of the proposed automation for fault-resilient continuum deformation coordination.

Transitions between the HDM and CEM is managed by commander agent $s \in \mathcal{V}_H$ that is positioned at

$$s = \underset{i \in \mathcal{V}_H}{\operatorname{arg \, min}} \left\{ (x_i(t) - \bar{x}_H(t))^2 + (y_i(t) - \bar{y}_H(t))^2 + (z_i(t) - \bar{z}_H(t))^2 \right\}$$
(15)

at time t where $\bar{\mu}_H(t) = \frac{1}{N_H(t)} \sum_{j=1}^{N_H} \mu_j(t)$ denotes the component $\mu \in \{x,y,z\}$ of the centroid of the healthy agents at time t. More specifically, the commander agent is responsible to accomplish the following tasks:

- 1) commanding on transition between HDM and CEM;
- determining leaders when the agent team enters the HDM mode:
- 3) detecting anomalous agents through characterizing agent deviation from the desired coordination.

Remark 4: The commander agent $s \in \mathcal{V}_H$ is assigned in an unsupervised fashion.

Assumption 1: This article studies resilience of continuum deformation coordination against vehicle failure. It is assumed that no deceptive or attacker agent exists in the containment domain $\Omega_{\rm con}$ at any time t.

Assumption 2: This article assumes that position information among the healthy agents is shared by a complete graph $\mathcal{G}_H(\mathcal{V}_H(t),\mathcal{E}_H(t))$ at any time t, where $\mathcal{E}_H(t)=\mathcal{V}_H(t)\times\mathcal{V}_H(t)$. Graph \mathcal{G}_H is different with proximity-based graph $\mathcal{G}_c(\mathcal{V},\mathcal{E})$ that is defined in Section IV-B for decentralized agent coordination at HDM.

Because agents are not deceptive (see Assumption 1), information communicated through graph \mathcal{G}_H is valid. Therefore, healthy and failed agents are assigned at any time t with no uncertainty.

IV. PROBLEM 1: PHYSICS-BASED MODELING OF HDM

At HDM, sets \mathcal{V} ($\mathcal{V} = \mathcal{V}_H$), \mathcal{V}_L , \mathcal{V}_F are expressed as follows:

$$\mathcal{V}_H = \{i_1, \dots, i_N\} \tag{16a}$$

$$\mathcal{V}_L = \{i_1, \dots, i_{n+1}\} \tag{16b}$$

$$\mathcal{V}_F = \{i_{n+2}, \dots, i_N\} \tag{16c}$$

where $i_j \in \mathcal{V}_H$ is the identification number of a healthy agent. Note that $i_j \in \mathcal{V}_H$ represents a leader if $j \in \{1, \dots, n+1\}$, and it represents a follower if $j \in \{n+2, \dots, N\}$.

A. Homogeneous Deformation Definition

A desired homogeneous deformation is defined by

$$i_i \in \mathcal{V}, \quad \mathbf{r}_{i_i,c,\text{HDM}}(t) = \mathbf{Q}(t)\mathbf{r}_{i_i,0,\text{HDM}} + \mathbf{d}(t)$$
 (17)

where $\mathbf{Q}(t)$ is the Jacobian matrix, $\mathbf{d}(t)$ is the rigid-body displacement vector, $\mathbf{r}_{i,0,\text{HDM}}$ is the reference position of agent $i_j \in \mathcal{V}(t)$ when HDM is continuously active. Homogeneous deformation is a linear transformation, thus, the global desired position of healthy $i_j \in \mathcal{V}$ can be expressed as a linear combination of the leaders' global desired positions by

$$i_j \in \mathcal{V}_H, \quad \mathbf{r}_{i_j,c,\text{HDM}} = \sum_{k=1}^{n+1} \alpha_{i_j,i_k} \mathbf{r}_{i_k,c}(t), \quad (18)$$

where

$$\begin{bmatrix} \alpha_{i_j,i_1} & \cdots & \alpha_{i_j,i_4} \end{bmatrix}^T$$

$$= \mathbf{\Lambda} \left(\mathbf{r}_{i_1,0,\text{HDM}}, \mathbf{r}_{i_2,0,\text{HDM}}, \mathbf{r}_{i_3,0,\text{HDM}}, \mathbf{r}_{i_4,0,\text{HDM}}^n, \mathbf{r}_{i_j,0,\text{HDM}}^n \right)$$
(19)

and

$$\mathbf{r}_{i_4,0,\text{HDM}}^n = \begin{cases} \mathbf{r}_{i_4,0,\text{HDM}} & n = 3\\ \mathbf{r}_{i_1,0,\text{HDM}} + \Xi \left(\mathbf{r}_{i_3,0,\text{HDM}} - \mathbf{r}_{i_1,0,\text{HDM}} \right) & n = 2\\ \times \left(\mathbf{r}_{i_2,0,\text{HDM}} - \mathbf{p}_{i_1,0,\text{HDM}} \right), \end{cases} \tag{20a}$$

$$\mathbf{r}_{i_j,0,\text{HDM}}^n = \begin{cases} \mathbf{r}_{i_j,0,\text{HDM}} & n = 3\\ \mathbf{r}_{i_j,0,\text{HDM}} - \left(\mathbf{r}_{i_j,0,\text{HDM}} \cdot \mathbf{n}_{1-4}\right) \mathbf{n}_{1-4} & n = 2. \end{cases}$$
(20b)

Note that $\mathbf{n}_{1-4} = \mathbf{n}_{1-4}(\mathbf{r}_{i_1,0,\text{HDM}}, \mathbf{r}_{i_2,0,\text{HDM}}, \mathbf{r}_{i_3,0,\text{HDM}})$ was previously defined in (5). Also, $\alpha_{i_1,i_4} = 0$ if n = 2 (See Proposition 1).

Equation (18) can be expressed in the form of (9) with shape matrix

$$\mathbf{H}_{i_j,\text{HDM}} = \begin{bmatrix} \mathbf{h}_{i_j,1,\text{HDM}} & \cdots & \mathbf{h}_{i_j,3(n+1),\text{HDM}} \end{bmatrix}$$
$$= \mathbf{I}_3 \otimes \begin{bmatrix} \alpha_{i_j,i_1} & \cdots & \alpha_{i_j,i_{n+1}} \end{bmatrix}$$
(21)

and generalized coordinate vector

$$\mathbf{q}_{\text{HDM}}(t) = \begin{bmatrix} q_{1,\text{HDM}}(t) \\ \vdots \\ q_{3(n+1),\text{HDM}}(t) \end{bmatrix}$$

$$= \text{vec} \begin{pmatrix} \begin{bmatrix} x_{i_1,c,\text{HDM}} & \cdots & x_{i_{n+1},c,\text{HDM}} \\ y_{i_1,c,\text{HDM}} & \cdots & y_{i_{n+1},c,\text{HDM}} \\ z_{i_1,c,\text{HDM}} & \cdots & z_{i_{n+1},c,\text{HDM}} \end{bmatrix}^T \end{pmatrix} \tag{22}$$

where \otimes is the Kronecher product symbol and $\operatorname{vec}(\cdot)$ is the matrix vectorization operator and $i_j \in \mathcal{V}_H$. Equation (22) implies that m = n(n+1) components of leaders' global trajectories define the HDM generalized coordinates $q_{1,\mathrm{HDM}}$ through $q_{m,\mathrm{HDM}}$.

In Sections IV-B, we present a leader–follower algorithm for acquisition of the global desired trajectory \mathbf{r}_{i_j} using the tetrahedralization introduced in Section II-B.

B. Continuum Deformation Acquisition

A desired homogeneous deformation, defined by n+1 leaders, is acquired by followers through local communication, where followers' communication weights are assigned based on agents' reference configuration. However, the MAS reference configuration is updated when the agent team recovers safety and transits from CEM to HDM. Hence, the agent team should be capable of determining the communications and followers' communication weights with no external supervision using the agent tetrahedralization, presented in Section II-B.

1) Classification of Agents as Leaders, Followers, Boundary Agents, and Interior Agents: Let node set \mathcal{V}_H be expressed as $\mathcal{V} = \mathcal{V}_B \bigcup \mathcal{V}_I$, where $\mathcal{V}_B = \{i_1, \dots, i_{m_B}\}$ and $\mathcal{V}_I = \{i_{m_B+1}, \dots, i_N\}$ define boundary and interior agents, respectively, $m_B \geq n+1$. Leaders are selected from boundary agents and assigned by solving the following optimization problem:

$$(i_{1}, \dots, i_{n+1}) = \underset{(j_{1}, \dots, j_{n+1}) \in \mathcal{V}_{H}^{n+1}}{\operatorname{argmin}} \|\mathbf{\Lambda}(\mathbf{r}_{j_{1}, 0, \text{HDM}}, \dots, \mathbf{r}_{j_{n+1}, 0, \text{HDM}}, \bar{\mathbf{r}}_{H, 0, \text{HDM}}^{n})\|_{2}^{2}$$

$$(23)$$

subject to

$$\varkappa_n\left(\mathbf{r}_{j_1,0,\text{HDM}},\dots,\mathbf{r}_{j_{n+1},0,\text{HDM}}\right) = n \tag{24a}$$

$$\mathbf{\Lambda}\left(\mathbf{r}_{j_1,0,\mathrm{HDM}},\mathbf{r}_{j_2,0,\mathrm{HDM}},\mathbf{r}_{j_3,0,\mathrm{HDM}},\mathbf{r}_{j_4,0,\mathrm{HDM}}^n,\bar{\mathbf{r}}_{H,0,\mathrm{HDM}}^n\right)$$

$$\geq \zeta \mathbf{1}_{4\times 1} \tag{24b}$$

where $\zeta>0$ is small $\bar{\mathbf{r}}_{H,0,\mathrm{HDM}}=\frac{1}{N}\sum_{j=1}^{N_H}\mathbf{r}_{i_j,0,\mathrm{HDM}}$ is the centroid of reference configuration of the healthy agents and $\bar{\mathbf{r}}_{H,0,\mathrm{HDM}}^n$ is assigned using (4). Constraint (24a) provides a necessary condition for constraint (24b), where (24b) ensures that $ar{\mathbf{r}}_{H,0,\mathrm{HDM}}^n$ is inside the leading simplex defined by n+1 leaders at the HDM.

In-neighbors of an interior follower $i_i \in \mathcal{V}_I$ is defined by set $\mathcal{N}_{i_i} = \{j_1^*, \dots, j_{n+1}^*\}, \text{ where }$

$$(j_1^*, \dots, j_{n+1}^*) = \underset{(j_1, \dots, j_{n+1}) \in \mathcal{V}_H^{n+1}}{\operatorname{argmin}}$$

$$\left\| \mathbf{\Lambda} \left(\mathbf{r}_{j_1,0,\text{HDM}}, \dots, \mathbf{r}_{j_{n+1},0,\text{HDM}}, \mathbf{r}_{i_j,0,\text{HDM}}^n \right) \right\|_2^2 \qquad (25)$$

subject to

$$\varkappa_n\left(\mathbf{r}_{j_1,0,\text{HDM}},\dots,\mathbf{r}_{j_{n+1},0,\text{HDM}}\right) = n \tag{26a}$$

$$\mathbf{\Lambda}\left(\mathbf{r}_{j_1,0,\mathrm{HDM}},\mathbf{r}_{j_2,0,\mathrm{HDM}},\mathbf{r}_{j_3,0,\mathrm{HDM}},\mathbf{r}_{j_4,0,\mathrm{HDM}}^n,\mathbf{r}_{i_j,0,\mathrm{HDM}}\right)$$

$$\geq \zeta \mathbf{1}_{4\times 1}.\tag{26b}$$

Every boundary follower agent $i_j \in \mathcal{V}_B \setminus \mathcal{V}_L$ communicates with n+1 leaders defined by \mathcal{V}_L . Therefore, $\mathcal{N}_{i_i} = \mathcal{V}_L$ defines the in-neighbor agents of vehicle $i_j \in \mathcal{V}_L \subset \mathcal{V}_B$.

Remark 5: While leaders are selected by the commander agent $s \in \mathcal{V}_H$, each follower assigns its own in-neighbors based on the agents' reference positions. Per Assumption 2, position information is accessible and communicated to all agents through the complete graph \mathcal{G}_H . Therefore, each follower assigns its own in-neighbors by solving the optimization problem (25) with constraints (26).

2) Followers' Interagent Communications: Followers' interagent communications are defined by coordination graph $\mathcal{G}_c(\mathcal{V}, \mathcal{E})$ with nodes \mathcal{V} ($\mathcal{V} = \mathcal{V}_H$) and edges $\mathcal{E} \subset \mathcal{V} \times \mathcal{V}$. Also, in-neighbor agents of agent $i \in \mathcal{V}$ are defined by $\mathcal{N}_i =$ $\{j|(j,i)\in\mathcal{E}\}.$

Defining $\mathcal{N}_{i_i} = \{j_1, \dots, j_{n+1}\}$, communication weight w_{i_j,j_k} is specified based on reference positions of follower $i_i \in \mathcal{V}_F$ and its in-neighbors as follows:

$$w_{i_j,j_k} = \lambda_k \left(\mathbf{r}_{j_1,0,\text{HDM}}, \mathbf{r}_{j_2,0,\text{HDM}}, \mathbf{r}_{j_3,0,\text{HDM}}, \mathbf{r}_{j_4,0,\text{HDM}}^n, \mathbf{r}_{i_j,0,\text{HDM}}^n \right)$$
(27)

for k = 1, ..., n + 1, where λ_k is the k-th entry of $\mathbf{\Lambda}(\mathbf{r}_{j_1,0,\text{HDM}},\mathbf{r}_{j_2,0,\text{HDM}},\mathbf{r}_{j_3,0,\text{HDM}},\mathbf{r}_{j_4,0,\text{HDM}}^n,\mathbf{r}_{i_j,0,\text{HDM}}^n),$

$$\mathbf{r}_{j_4,0,\text{HDM}}^n = \begin{cases} \mathbf{r}_{j_4,0,\text{HDM}} & n = 3\\ \mathbf{r}_{j_1,0,\text{HDM}} + \Xi \left(\mathbf{r}_{j_3,0,\text{HDM}} - \mathbf{r}_{j_1,0,\text{HDM}} \right) & n = 2,\\ \times \left(\mathbf{r}_{j_2,0,\text{HDM}} - \mathbf{r}_{j_1,0,\text{HDM}} \right) & (28a) \end{cases} \qquad \mathbf{Y}_{c,\text{HDM}}(t) = \mathbf{vec} \left(\left[\mathbf{r}_{i_1,c,\text{HDM}}(t) \cdots \mathbf{r}_{i_N,c,\text{HDM}}(t) \right]^T \right)$$

$$\mathbf{r}_{i,0,\text{HDM}}^{n} = \begin{cases} \mathbf{r}_{i,0,\text{HDM}} & n = 3\\ \mathbf{r}_{i,0,\text{HDM}} - (\mathbf{r}_{i,0,\text{HDM}} \cdot \mathbf{n}_{1-4}) \mathbf{n}_{1-4} & n = 2 \end{cases}$$
(28b)

and $\mathbf{n}_{1-4} = \mathbf{n}_{1-4}(\mathbf{r}_{j_1,0,\text{HDM}},\mathbf{r}_{j_2,0,\text{HDM}},\mathbf{r}_{j_3,0,\text{HDM}})$ is determined using (5). Given followers' communication weights, the weight matrix $\mathbf{W} = [W_{jh}] \in \mathbb{R}^{N \times N}$ is defined as follows:

$$W_{jh} = \begin{cases} w_{i_j, i_h} & i_h \in \mathcal{N}_{i_j} \land i_j \in \mathcal{V}_F \\ 0 & \text{otherwise.} \end{cases}$$
 (29)

Matrix W can be partitioned as follows:

$$\mathbf{W} = \begin{bmatrix} \mathbf{0} & \mathbf{0} & \mathbf{0} \\ \mathbf{B}_1 & \mathbf{0} & \mathbf{0} \\ \mathbf{B}_2 & \mathbf{C} & \mathbf{A} \end{bmatrix}$$
 (30)

where $\mathbf{B}_1 \in \mathbb{R}^{(m_B-n-1)\times(n+1)}$, $\mathbf{B}_2 \in \mathbb{R}^{(N-m_B)\times(n+1)}$, $\mathbf{C} \in \mathbb{R}^{(N-m_B)\times(m_B-n-1)}$, and $\mathbf{A} \in \mathbb{R}^{(N-m_B)\times(N-m_B)}$ are non negative matrices.

Theorem 1: For an arbitrary reference configuration of agents, if i) first, coordination graph $\mathcal{G}_c(\mathcal{V}, \mathcal{E})$ defines at least one directed path from every leader $i_h \in \mathcal{V}_L$ $(h = 1, \dots, n+1)$ toward every follower $i_j \in \mathcal{V}_F$ $(j = n + 2, \dots, N)$ and followers' communication weights are obtained by (27); ii) second, leaders and follower are assigned by solving (23) through (26); and iii) third, followers' communication weights are consistent with agents' reference positions and assigned by (27), then the following properties hold:

1) Matrix

$$\mathbf{D} = -\mathbf{I} + \mathbf{W} \tag{31}$$

is Hurwitz and every row of matrix $\mathbf{W}_L = -\mathbf{D}^{-1}\mathbf{L}_0$ sums up to 1, where $\mathbf{L}_0 = \begin{bmatrix} \mathbf{I}_{n+1} & \mathbf{0} \end{bmatrix}^T \in \mathbb{R}^{N \times (n+1)}$ and

$$\mathbf{W}_{L} = \begin{bmatrix} 1 & \cdots & 0 \\ \vdots & \ddots & \vdots \\ 0 & \cdots & 1 \\ \alpha_{i_{n+2},i_{1}} & \cdots & \alpha_{i_{n+2},i_{n+1}} \\ \vdots & \ddots & \vdots \\ \alpha_{i_{N},i_{1}} & \cdots & \alpha_{i_{N},i_{n+1}} \end{bmatrix} \in \mathbb{R}^{N \times (n+1)}.$$
(32)

2) Let

$$\mathbf{Y}(t) = \mathbf{vec} \left(\begin{bmatrix} \mathbf{r}_{i_1}(t) & \cdots & \mathbf{r}_{i_N}(t) \end{bmatrix}^T \right) \in \mathbb{R}^{3N \times 1}$$
(33a)

$$\mathbf{Y}_d(t) = \mathbf{vec} \left(\begin{bmatrix} \mathbf{r}_{i_1,d}(t) & \cdots & \mathbf{r}_{i_N,d}(t) \end{bmatrix}^T \right) \in \mathbb{R}^{3N \times 1}$$
(33b)

$$\mathbf{Y}_{c,\text{HDM}}(t) = \mathbf{vec} \left(\left[\mathbf{r}_{i_1, c, \text{HDM}}(t) \cdots \mathbf{r}_{i_N, c, \text{HDM}}(t) \right]^T \right)$$

$$\in \mathbb{R}^{3N \times 1}$$
(33c)

be the MAS actual desired trajectory, MAS local desired trajectory, and MAS global desired trajectory, respectively. Then,

$$\mathbf{Y}_d(t) - \mathbf{Y}(t) = (\mathbf{I}_3 \otimes \mathbf{D}) (\mathbf{Y}(t) - \mathbf{Y}_{c,HDM}(t))$$
 (34)

at any time t.

As shown in Fig. 2, \mathbf{Y}_d and \mathbf{Y} are the input and output of the MAS control system. Equation (34) relates the local error vector $\mathbf{E}_d = \mathbf{Y}_d - \mathbf{Y}$ to the global error vector $\mathbf{E}_{c,\text{HDM}} = \mathbf{Y} - \mathbf{Y}_{c,\text{HDM}}(t)$ at any time t. Although, no follower agent knows its global desired trajectory, the global error vector $\mathbf{E}_{c,\text{HDM}}$ remains bounded if \mathbf{Y} stably tracks $\mathbf{Y}_d(t)$.

Theorem 1 is applied in Section IV-B3 to provide a guarantee condition for convergence of the proposed decentralized proximity-based continuum deformation coordination.

3) Trajectory Tracking: The objective of the trajectory control is to ensure deviation of actual position of every agent from its global desired trajectory is bounded while each agent only accesses its local desired trajectory, and every healthy agent $i_j \in \mathcal{V}$ $(j=1,\ldots,N)$ chooses a proper control input \mathbf{u}_i such that

$$\forall t \quad i_j \in \mathcal{V}, j = 1, \dots, N, \qquad \|\mathbf{r}_{i_j}(t) - \mathbf{r}_{i_j,d}(t)\| \le \hat{\Delta}. \tag{35}$$

Lemma 1 and Theorem 2 are provided below to relate the local upper-bound error $\hat{\Delta}$ to the global upper-bound error Δ at any time t, where

$$\forall t, i_j \in \mathcal{V}, j = 1, \dots, N, \qquad \|\mathbf{r}_{i_j}(t) - \mathbf{r}_{i_j, c, \text{HDM}}(t)\| \le \Delta.$$
(36)

Lemma 1: Matrix \mathbf{D}^{-1} is nonpositive.

Theorem 2: Assume control inputs \mathbf{u}_{i_1} through \mathbf{u}_{i_N} are designed such that

$$j = 1, \dots, N, \forall_{i_j} \in \mathcal{V}, \forall \mu \in \{x, y, z\}, \ \left| \mu_{i_j} - \mu_{i_j, d} \right| \leq \hat{\Delta}_{\mu}$$
(37)

where μ_{i_j} and $\mu_{i_j,d} = \sum_{i_h \in \mathcal{N}_{i_j}} w_{i_j,i_h} \mu_h$ are the component $\mu \in \{x,y,z\}$ of the actual and local desired positions of vehicle $i_j \in \mathcal{V}$; communication weight w_{i_j,i_h} is obtained using (27).

Then, (36) is satisfied if
$$\Delta = \Phi_{\max} \hat{\Delta}$$
, $\hat{\Delta} = \sqrt{\hat{\Delta}_x^2 + \hat{\Delta}_y^2 + \hat{\Delta}_z^2}$ and $\Phi_{\max} = -\max_{x} (-\sum_{j=1}^{N} \mathbf{D}_{lj}^{-1})$.

Theorem 2 specifies an upper limit the agent deviation from the desired coordination defined at HDM, assuming every agent is enclosed by a ball of radius ϵ . Interagent collision avoidance is guaranteed at HDM, if the following inequality constraint is satisfied at any time t [30]:

$$\forall t \quad \min\{\sigma_1(t), \sigma_2(t), \sigma_3(t)\} \ge \frac{\Delta + \epsilon}{\frac{d_{\min}}{2} + \epsilon}$$
 (38)

where d_{\min} is the minimum separation distance between every vehicle pair in the reference configuration.

V. PROBLEM 2: PHYSICS-BASED MODELING OF CEM

CEM is activated when there exists at least one agent experiencing a failure or anomaly in containment domain $\Omega_{\rm con}$. Therefore, $N_H(t) < N(t)$ at time t and "healthy" and "anomalous"

agents are defined by sets

$$\mathcal{V}_H = \{i_1, \dots, i_{N_H}\} \tag{39a}$$

$$V_A = \{i_{N_H+1}, \dots, i_N\},$$
 (39b)

respectively. At CEM, coordination of the healthy agents are defined by an "ideal fluid flow" pattern, where the failed agent(s) are wrapped with an exclusion zone and healthy agents must be routed around. Without loss of generality, potential function ϕ and stream function ψ are determined by combining "Uniform" and "Doublet" flows:

$$\phi(x, y, t) = \phi_U(x, y, t) + \phi_D(x, y, t)$$

$$\psi(x, y, t) = \psi_U(x, y, t) + \psi_D(x, y, t)$$

where the subscripts U and D are associated with "Uniform" and "Doublet," respectively. For the uniform flow pattern,

$$\phi_U(x, y, t) = u_\infty(t) \left(x \cos \theta_\infty(t) + y \sin \theta_\infty(t) \right) \tag{40a}$$

$$\psi_U(x, y, t) = u_\infty(t) \left(-x \sin \theta_\infty(t) + y \cos \theta_\infty(t) \right)$$
 (40b)

define the potential and stream fields, respectively, where $u_{\infty}(t)$ and $\theta_{\infty}(t)$ are the design parameters. Furthermore,

$$\phi_D = \sum_{l=N_H+1}^{N} \phi_{D,i_l}$$
 and $\psi_D = \sum_{l=N_H+1}^{N} \psi_{D,i_l}$

define potential and stream fields of the Doublet flow, respectively, where

$$\phi_{D,i_l}$$
 =

$$\frac{\delta_{i_l}(t) \left[\cos \gamma_{i_l}(t) \left(x - a_{i_l}(t)\right) + \sin \gamma_{i_l}(t) \left(y - b_{i_l}(t)\right)\right]}{\left(x - a_{i_l}(t)\right)^2 + \left(y - b_{i_l}(t)\right)^2},$$
(41a)

 $\psi_{D,i_I} =$

$$\frac{\delta_{i_{l}}(t)\left[\sin\gamma_{i_{l}}(t)\left(x-a_{i_{l}}(t)\right)-\cos\gamma_{i_{l}}(t)\left(y-b_{i_{l}}(t)\right)\right]}{\left(x-a_{i_{l}}(t)\right)^{2}+\left(y-b_{i_{l}}(t)\right)^{2}},$$
(41b)

 $\gamma_{i_l}(t)$ is known at time t and δ_{i_l} , a_{i_l} , and b_{i_l} are design parameters specifying the geometry and location of anomalous/failed agent $i_l \in \mathcal{V}_A$ in the motion space where $l \in \{N_H+1,\ldots,N\}$. By treating agent coordination as ideal fluid flow, we can exclude failed agent $i_l \in \mathcal{V}_A$ by wrapping it with a closed surface $\psi(x,y,t)=\psi_{h,0}$, where $\psi_{i_l,0}$ is constant ($l=N_H+1,\ldots,N$). Furthermore, healthy vehicle $i_j \in \mathcal{V}_H$ moves along the global desired trajectory defined by (12), where $\psi_{i_j,0}$ is assigned based on position of vehicle $i_j \in \mathcal{V}_H$ at the time the cooperative team enters the CEM and $j=\{1,\ldots,N_H\}$.

Theorem 3: Suppose $\mathbf{J}(x_{i_j,c,\text{CEM}},y_{i_j,c,\text{CEM}},t)$ is the Jacobian matrix defined by (14), and the desired trajectory of every agent $i_j \in \mathcal{V}_H$ satisfies (13). Define

$$\mathbf{H}_{s,i_{j}} = -\frac{1}{\left|\mathbf{J}\left(x_{i_{j},c,\text{CEM}}, y_{i_{j},c,\text{CEM}}, t\right)\right|} \times \begin{bmatrix} \frac{\partial \psi}{\partial y_{i_{j},c,\text{CEM}}} \\ -\frac{\partial \psi}{\partial x_{i_{j},c,\text{CEM}}} \end{bmatrix} \begin{bmatrix} \frac{\partial \phi}{\partial u_{\infty}} & \frac{\partial \phi}{\partial \theta_{\infty}}, \end{bmatrix}$$
(42a)

$$\mathbf{H}_{a,i_{j},i_{l}} = -\frac{1}{\left|\mathbf{J}\left(x_{i_{j},c,\text{CEM}}, y_{i_{j},c,\text{CEM}}, t\right)\right|} \times \begin{bmatrix} \frac{\partial \psi}{\partial y_{i_{j},c,\text{CEM}}} \\ -\frac{\partial \psi}{\partial x_{i_{j},c,\text{CEM}}} \end{bmatrix} \begin{bmatrix} \frac{\partial \phi}{\partial a_{i_{l}}} & \frac{\partial \phi}{\partial b_{i_{l}}} & \frac{\partial \phi}{\partial \delta_{i_{l}}} \end{bmatrix}$$
(42b)

$$\mathbf{H}_{T,i_{j}} = \frac{1}{\left|\mathbf{J}\left(x_{i_{j},c,\text{CEM}}, y_{i_{j},c,\text{CEM}}, t\right)\right|} \times \left[\frac{\partial \psi}{\partial y_{i_{j},c,\text{CEM}}} - \frac{\partial \psi}{\partial x_{i_{j},c,\text{CEM}}}\right]^{T}, \tag{42c}$$

$$\dot{\mathbf{q}}_{c,\text{CEM}} = \left[\dot{u}_{\infty}\dot{\theta}_{\infty}\right]^{T},\tag{42d}$$

$$\dot{\mathbf{q}}_{u,\text{CEM}} = \left[\dot{a}_{i_{N_H+1}} \dot{b}_{i_{N_H+1}} \dot{\delta}_{i_{N_H+1}} \cdots \dot{a}_{i_N} \dot{b}_{i_N} \dot{\delta}_{i_N} \right]^T$$
. (42e)

Then, the CEM global desired trajectory can be defined by (9), where $\gamma = \text{CEM}$,

$$\dot{\mathbf{q}}_{\text{CEM}} = \begin{bmatrix} \dot{\mathbf{q}}_{c,\text{CEM}} \\ \dot{\mathbf{q}}_{u,\text{CEM}} \\ v_{\phi} \end{bmatrix} \in \mathbb{R}^{(3+3(N-N_H))\times 1}, \tag{43a}$$

$$\mathbf{H}_{i_j,\text{CEM}} = \begin{bmatrix} 1 & 0 \\ 0 & 1 \\ \frac{\partial z_{i_j,c,\text{CEM}}}{\partial x_{i_j,c,\text{CEM}}} & \frac{\partial z_{i_j,c,\text{CEM}}}{\partial y_{i_j,c,\text{CEM}}} \end{bmatrix}$$

$$\begin{bmatrix} \mathbf{H}_s & \mathbf{H}_{a,i_{N_H+1}} & \cdots & \mathbf{H}_{a,i_N} & \mathbf{H}_{T,i_j} \end{bmatrix} \tag{43b}$$

for every agent $i_j \in \mathcal{V}_H$, $z_{i_j,c,\text{CEM}} = z(x_{i_j,c,\text{CEM}}, y_{i_j,c,\text{CEM}}, t)$ and $v_\phi = \frac{\partial \phi}{\partial t}$ is the desired sliding speed of healthy vehicles along their desired stream lines.

Parameters \dot{u}_{∞} , $\dot{\theta}_{\infty}$, $\dot{\delta}_{i_l}$, \dot{a}_{i_l} , \dot{b}_{i_l} ($i_l \in \mathcal{V}_A$ and $l \in \{N_H + 1, \ldots, N\}$), obtained by taking time derivative from the generalized coordinates, define group desired coordination for CEM. Note that \dot{u}_{∞} , $\dot{\theta}_{\infty}$, and \dot{v}_{ϕ} can be designed so that the ideal fluid flow coordination is optimized. However, the remaining design parameters are uncontrolled.

Remark 6: In general, design parameters \dot{u}_{∞} , θ_{∞} , δ_{i_l} , \dot{a}_{i_l} , \dot{b}_{i_l} ($i_l \in \mathcal{V}_A$ and $l \in \{N_H+1,\ldots,N\}$) can vary with time. However, this article concentrates only on the steady-state CEM, which will be achieved when \dot{u}_{∞} , $\dot{\theta}_{\infty}$, $\dot{\delta}_{i_l}$, \dot{a}_{i_l} , \dot{b}_{i_l} are all zeros. Therefore, potential and stream functions are defined by (40), and (41) simplifies to

$$i_{j} \in \mathcal{V}_{H}, j = 1, \dots, N_{H},$$

$$\begin{bmatrix} \dot{x}_{i_{j},c,\text{CEM}} \\ \dot{y}_{i_{j},c,\text{CEM}} \\ \dot{z}_{i_{j},c,\text{CEM}} \end{bmatrix} = \begin{bmatrix} 1 & 0 \\ 0 & 1 \\ \frac{\partial z_{i_{j},c,\text{CEM}}}{\partial x_{i_{j},c,\text{CEM}}} & \frac{\partial z_{i_{j},c,\text{CEM}}}{\partial y_{i_{j},c,\text{CEM}}} \end{bmatrix} \mathbf{H}_{T,i_{j}} v_{\phi}. \quad (44)$$

This requires an assumption for this work that the failed vehicle $i_l \in \mathcal{V}_A$ remains inside a predictable closed domain $\mathcal{U} = \bigcup_{l=N_H+1}^N \mathcal{U}_{i_l}$ with time-invariant geometry, until the time the failed agent is no longer in containment domain Ω_{con} . This condition can be assured by choosing a sufficiently large value for

the generalized coordinate v_{ϕ} such that the anomalous agent(s) do not leave $\mathcal U$ while the healthy agents move fast enough along the recovery stream lines.

VI. PROBLEM 3: CONTINUUM DEFORMATION ANOMALY MANAGEMENT

This section develops a hybrid model to manage transitions between CEM and HDM. Section VI-A develops a distributed approach to detect a vehicle failure/anomaly. This is followed by specification of transition conditions in Section VI-B.

A. Anomaly Detection

We first present a distributed model to detect situations in which agents have failed or are no longer cooperative. We then consider these agents anomalous or failed and add them to anomalous agent set \mathcal{V}_A .

Consider an n-D homogeneous deformation where interior follower $i_j \in \mathcal{V}_I$ ($j = m_B + 1, \ldots, N$) knows its own position and positions of in-neighbor agents $\mathcal{N}_{i_j} = \{j_1, \ldots, j_{n+1}\}$. Let actual position $\mathbf{r}_{i_j}(t)$ be defined by convex combination of agent i_j 's in-neighbors by

$$j = m_B + 1, \dots, N, i_j \in \mathcal{V}_I, \quad \mathbf{r}_{i_j}(t) = \sum_{k=1}^{n+1} \varpi_{i_j, j_k}(t) \mathbf{r}_{j_k}(t).$$

$$(45)$$

where $N_H=N$ and ϖ_{i,j_1} through $\varpi_{i,j_{n+1}}$ are called *transient* weights. If $\varkappa_n(\mathbf{r}_{j_1}(t),\ldots,\mathbf{r}_{j_{n+1}}(t))=n$, transient weights ϖ_{i_j,j_1} through $\varpi_{i_j,j_{n+1}}$ can be assigned based on agents' actual positions as follows:

$$\begin{bmatrix} \varpi_{i_j,j_1}(t) & \cdots & \varpi_{i_j,j_4}(t) \end{bmatrix}^T = \mathbf{\Lambda} \left(\mathbf{r}_{j_1}, \mathbf{r}_{j_2}, \mathbf{r}_{j_3}, \mathbf{r}_{j_4}^n, \mathbf{r}_{i_j}^n \right)$$
(46)

where

$$\mathbf{r}_{j_4}^n(t) = \begin{cases} \mathbf{r}_{j_4}(t) & n = 3\\ \mathbf{r}_{j_1} + \Xi \left(\mathbf{r}_{j_3} - \mathbf{r}_{j_1}\right) \times \left(\mathbf{r}_{j_2} - \mathbf{r}_{j_1}\right) & n = 2, \end{cases}$$
(47a)

$$\mathbf{r}_{i,0}^{n}(t) = \begin{cases} \mathbf{r}_{i} & n = 3\\ \mathbf{r}_{i} - (\mathbf{r}_{i} \cdot \mathbf{n}_{1-4}) \mathbf{n}_{1-4} & n = 2, \end{cases}$$
(47b)

and $\mathbf{n}_{1-4} = \mathbf{n}_{1-4}(\mathbf{r}_{j_1}, \mathbf{r}_{j_2}, \mathbf{r}_{j_3})$ is determined based on agents' actual positions using (5) for n = 2.

Geometric Interpretation of Transient Weights: Let $d_{i_j,j_2,j_3}(t)$, $d_{i_j,j_3,j_1}(t)$, and $d_{i_j,j_1,j_2}(t)$ denote distances of point $i_j \in \mathcal{V}_I$ $(j=m_B,\ldots,N_H)$ from the triangle sides $j_2-j_3,\,j_3-j_1$, and j_1-j_2 , respectively. Assume $l_{j_1,j_2,j_3}(t)$, $l_{j_2,j_3,j_1}(t)$, and $l_{j_3,j_1,j_2}(t)$ determine distances of vertices j_1 , j_2 , and j_3 from the triangle sides $j_2-j_3,\,j_3-j_1$, and j_1-j_2 , respectively. Then,

$$\begin{split} \varpi_{i_j,j_1}(t) &= \frac{d_{i_j,j_2,j_3}(t)}{l_{j_1,j_2,j_3}(t)}, \varpi_{i_j,j_2}(t) = \frac{d_{i_j,j_3,j_1}(t)}{l_{j_2,j_3,j_1}(t)}, \varpi_{i_j,j_3}(t) \\ &= \frac{d_{i_j,j_1,j_2}(t)}{l_{j_3,j_1,j_2}(t)}. \end{split}$$

Geometric representations of $d_{i_j,j_2j_3}(t)$ and $l_{j_1,j_2j_3}(t)$ are shown in Fig. 3(a) for n=2.

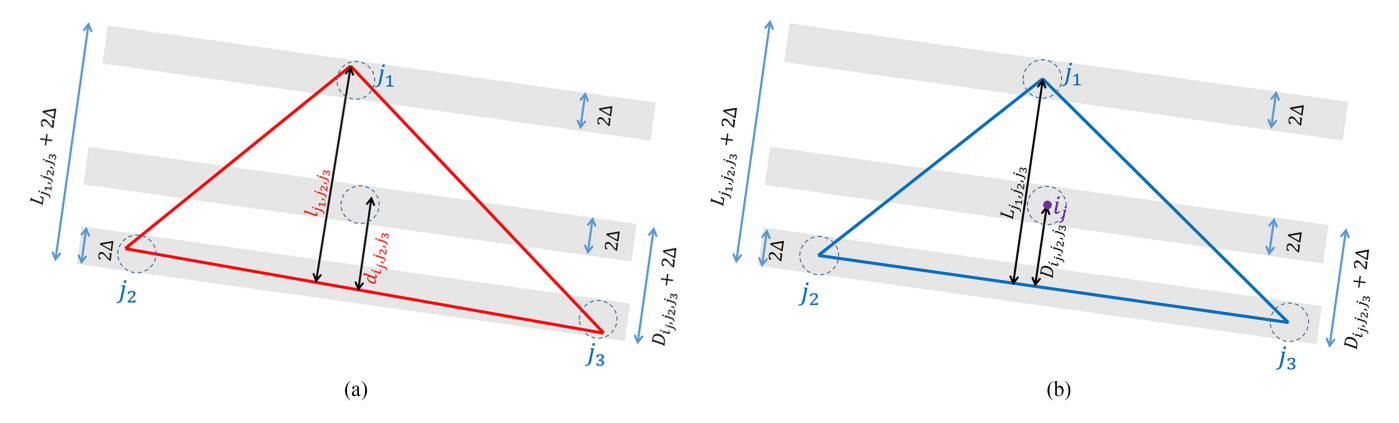


Fig. 3. (a) "Actual" triangle constructed by the actual positions of agents j_1 , j_2 , and j_3 at time t. (b) "Desired" triangle given by the global desired positions of agents j_1 , j_2 , and j_3 at time t.

For n=3, $d_{i_{j},j_{2},j_{3},j_{4}}(t)$, $d_{i_{j},j_{3},j_{4}j_{1}}(t)$, $d_{i_{j},j_{4},j_{1},j_{2}}(t)$, and $d_{i_{j},j_{1},j_{2},j_{3}}(t)$ denote distance of point $i_{j} \in \mathcal{V}_{I}$ from the triangular surfaces $j_{2}-j_{3}-j_{4}$, $j_{3}-j_{4}-j_{1}$, $j_{4}-j_{1}-j_{2}$, and $j_{1}-j_{2}-j_{3}$, respectively. Assume $l_{j_{1},j_{2},j_{3},j_{4}}(t)$, $l_{j_{2},j_{3},j_{4},j_{1}}(t)$, $l_{j_{3},j_{4},j_{1},j_{2}}(t)$, and $l_{j_{4},j_{1},j_{2},j_{3}}(t)$ determine distance of vertices j_{1} , j_{2} , j_{3} , and j_{4} , from the triangular surfaces $j_{2}-j_{3}-j_{4}$, $j_{3}-j_{4}-j_{1}$, $j_{4}-j_{1}-j_{2}$, and $j_{1}-j_{2}-j_{3}$, respectively. Then,

$$\begin{split} \varpi_{i_j,j_1}(t) &= \frac{d_{i_j,j_2,j_3,j_4}(t)}{l_{j_1,j_2,j_3,j_4}(t)}, \varpi_{i_j,j_2}(t) = \frac{d_{i_j,j_3,j_4,j_1}(t)}{l_{j_2,j_3,j_4,j_1}(t)}, \\ \varpi_{i_j,j_3}(t) &= \frac{d_{i_j,j_4,j_1,j_2}(t)}{l_{j_3,j_4,j_1,j_2}(t)}, \varpi_{i_j,j_4}(t) = \frac{d_{i_j,j_1,j_2,j_3}(t)}{l_{i_j,j_1,j_2,j_3}(t)}. \end{split}$$

Theorem 4: Assume HDM collective motion is guided by n+1 leaders, defined by \mathcal{V}_L , every follower $i_j \in \mathcal{V}_I$, communicates with n+1 in-neighbor agents, defined by $\mathcal{N}_{i_j} = \{j_1,\ldots,j_{n+1}\}$, where follower i_j 's in-neighbors form an n-D simplex at time t. If deviation of every agent $i_j \in \mathcal{V}_I$ from the global desired position $\mathbf{r}_{i_j,c,\mathrm{HDM}}$ is less than Δ at time t ($\|\mathbf{r}_{i_j}(t)-\mathbf{r}_{i_j,c,\mathrm{HDM}}(t)\| \leq \Delta$), then

$$\varpi_{i_{j},j_{1}}^{\min}(t) \le w_{i_{j},j_{1}} \le \varpi_{i_{j},j_{1}}^{\max}(t)$$
 (48)

at t, where $w_{i_j,j}$ is constant communication weight of a follower $i_j \in \mathcal{V}_I$ with in-neighbor j_1 assigned by (27),

$$\varpi_{i_{j},j_{1}}^{\min}(t) = \begin{cases}
\frac{d_{i_{j},j_{2},j_{3}}(t) - \Delta}{l_{j_{1},j_{2},j_{3}}(t) + 2\Delta} & n = 2 \\
\frac{d_{i_{j},j_{2},j_{3}}(t) + 2\Delta}{l_{j_{1},j_{2},j_{3},j_{4}}(t) - \Delta} & n = 3,
\end{cases}$$

$$\varpi_{i_{j},j_{1}}^{\max}(t) = \begin{cases}
\frac{d_{i_{j},j_{2},j_{3},j_{4}}(t) + 2\Delta}{l_{j_{1},j_{2},j_{3},j_{4}}(t) + 2\Delta} & n = 2 \\
\frac{d_{i_{j},j_{2},j_{3},j_{4}}(t) + 2\Delta}{l_{j_{1},j_{2},j_{3},j_{4}}(t) + 2\Delta} & n = 3
\end{cases}$$

specify lower and upper bounds for transient weight $\varpi_{i,j_1}(t)$ at time t.

Theorem 4 implies that the HDM mode is active only if the following condition is satisfied:

$$\forall i_j \in \mathcal{V}_I, k = 1, \dots, n+1,$$

$$\varpi_{i_j, j_k}^{\min}(t) \le w_{i_j, j_k} \le \varpi_{i_j, j_k}^{\max}(t) \qquad (\Psi_{i_j, j_k})$$

where $\mathcal{N}_{i_j} = \{j_1, \dots, j_{n+1}\}$ defines in-neighbors of agent $i_j \in \mathcal{V}_I$. Therefore, if $\bigwedge_{j=m_B+1}^{N(t)} \bigwedge_{k=1}^{n+1} \Psi_{i_j,j_k}$ is satisfied at time t, HDM is active. Otherwise, an anomaly is detected. Additionally, disjoint sets \mathcal{V}_H and \mathcal{V}_A are defined as follows:

$$\mathcal{V}_{H}(t) = \left\{ i_{j} \in \mathcal{V}(t) \middle| \bigwedge_{j=m_{B}+1}^{N(t)} \bigwedge_{k=1}^{n+1} \Psi_{i_{j},j_{k}} \text{ is satisfied.} \right\}, \tag{49a}$$

$$\mathcal{V}_A(t) = \mathcal{V}(t) \setminus \mathcal{V}_H(t).$$
 (49b)

Because u_{∞} , θ_{∞} , Δ_{i_l} , a_{i_l} , and b_{i_l} are constant ($i_l \in \mathcal{V}_A$ and $l = N_H + 1, \ldots N$), healthy agents need to know these design parameters only at the time they enter the CEM. Afterward, anomalous agents are wrapped and excluded from the safe motion space, and each healthy agent is capable to assign its global desired trajectory using (44) in Remark 6.

B. Vehicle Anomaly/Failure Management

Fig. 2 illustrates how vehicle failure can be managed by transition between "HDM" and "CEM". The following procedure is proposed.

- 1) Define containment domain $\Omega_{con}(\mathbf{r}, \mathbf{r}_{con}(t))$.
- 2) If there exists at least one failed agent inside the containment domain $\Omega_{\rm con}({\bf r},{\bf r}_{\rm con}(t))$, then

$$\bigwedge_{j=m_B+1}^{N(t)} \bigwedge_{k=1}^{n+1} \Psi_{i_j,j_k}$$

is not satisfied and CEM is activated.

3) If agents contained by $\Omega_{\rm con}({\bf r},{\bf r}_{\rm con}(t))$ are all healthy, then $\bigwedge_{j=m_B+1}^{N(t)} \bigwedge_{k=1}^{n+1} \Psi_{i_j,j_k}$ is *satisfied* which, in turn, implies that $\mathcal{V}_A=\emptyset$ and HDM is active.

VII. SIMULATION RESULTS

Consider collective motion in a 2-D plane with invariant z components for all agents at all times t. Suppose a multiagent team consisting of 22 vehicles is deployed with the initial formation shown in Fig. 4(a). The containment domain $\Omega_{\rm com}$ is defined for this case study as $\Omega_{\rm con} = \|{\bf r} - {\bf r}_{\rm con}\|_1 \le 40$, where

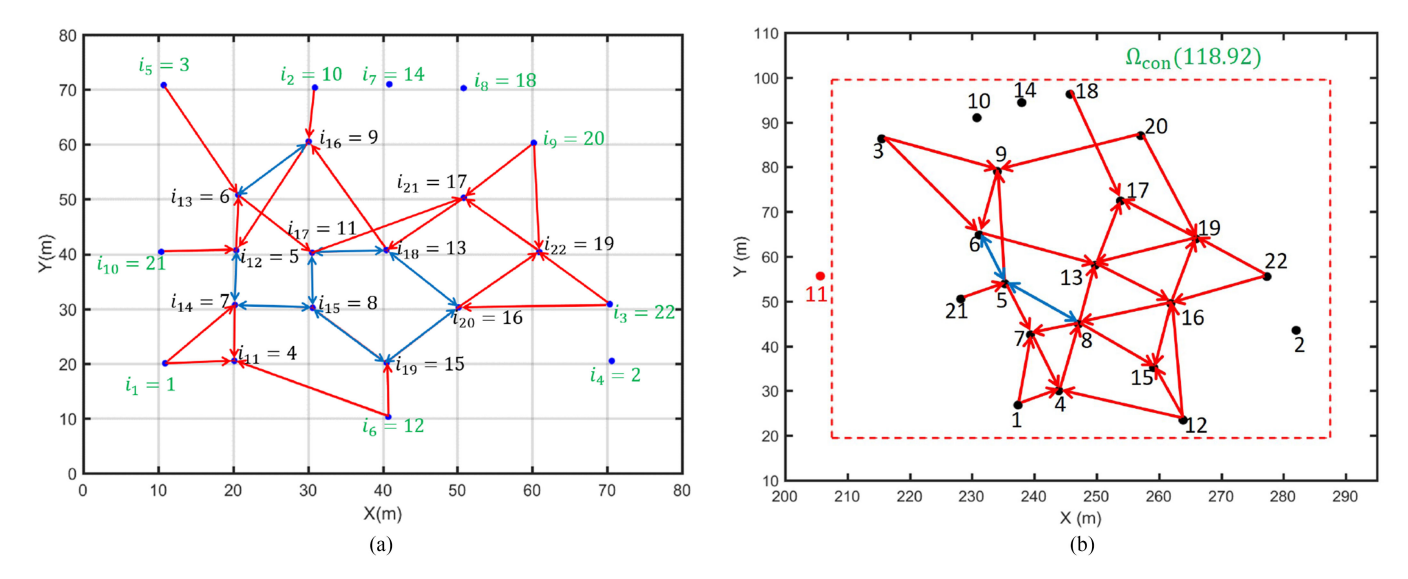


Fig. 4. (a) Reference configuration of the agents at initial t=0. (b) Reference configuration of the agents at t=118.92 s when safety is recovered and agent 11 is no longer inside the containment box $\Omega_{\rm con}$.

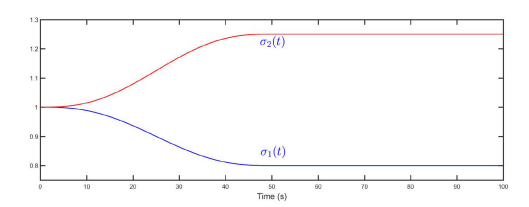


Fig. 5. Homogeneous deformation eigenvalues σ_1 and σ_2 versus time for $t \in [0, 100]$ s.

 $\begin{aligned} \mathbf{r}_{\mathrm{con}}(t) &= \frac{1}{N(t)} \sum_{i \in \mathcal{V}_H} \mathbf{r}_i(t) \ \text{ and } \| \cdot \|_1 \ \text{ denotes the 1-norm.} \\ \text{Therefore, } \Omega_{\mathrm{con}} \text{ is a box with a side length of 80 m. Without loss of generality, it is assumed that every agent is a single integrator.} \\ \text{The position of each agent } i \text{ is updated by} \end{aligned}$

$$i \in \mathcal{V}, \quad \dot{\mathbf{r}}_i = g(\mathbf{r}_{i,d} - \mathbf{r}_i)$$
 (50)

where g = 25 is constant, \mathbf{r}_i is the actual position of agent i, and local desired position $\mathbf{r}_{i,d}$ was defined in (1).

A. Motion Phase 1 (HDM)

Team collective motion is defined by a homogeneous transformation over $t \in [0, 100]$, where agents are all healthy. Agents $i_1 = 1, i_2 = 2$, and $i_3 = 3$ are the leaders defining the homogeneous transformation. Given leaders' desired trajectories, eigenvalues of the desired homogeneous deformation coordination, denoted by σ_1 and σ_2 , are plotted versus time in Fig. 5. Note that $\sigma_3(t) = 1$ at any time t because agents are treated as particles of a 2-D continuum and the desired homogenous deformation coordination is also 2D. Follower vehicles apply the communication graph shown in Fig. 4(a) to acquire the desired coordination by local communication. The communication graph is strictly 3-reachable per Section IV. Given initial positions of all agents, every follower chooses three in-neighbor agents using the approach described in Section IV. Consequently, the

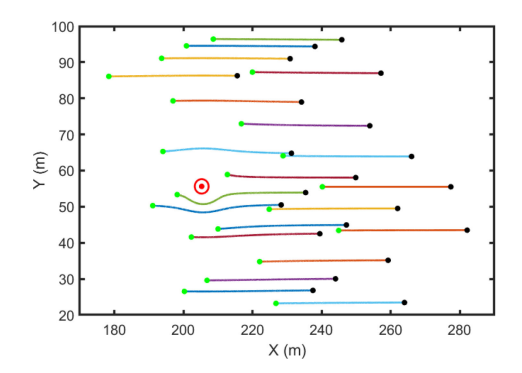


Fig. 6. Paths of healthy agents over $t \in [100.35, 118.92]$ when CEM is active. The green and block markers show positions of agents at times 100.35 and 118.92, respectively. Failed agent 11 is wrapped by a disk of radius 2 m centered at (205.26,55.62) when CEM is active.

graph shown in Fig. 4 assigns interagent communication, where followers' communication weights are consistent with agents' positions at reference time t=0 and obtained by (27). As shown in Fig. 7, HDM is active before an anomaly situation arises at time $t=100~\rm s$.

B. Motion Phase 2 (CEM)

Suppose agent 11 fails at time t=100. In Appendix C, it is described how this failure is quickly detected by the team using the distributed failure detection method developed in Section VI. Therefore, CEM is activated, and healthy agent coordination is treated as an ideal fluid flow after 100.35 s. The ideal fluid flow coordination is defined by combining "Uniform" and "Doublet" flow patterns. Anomalous agent 11 is wrapped by a disk of radius a=2 m resulted from choosing $u_{\infty}=10$ and $\delta=40$, i.e., $a=\sqrt{\frac{\delta}{u_{\infty}}}=2$ m. The remaining healthy agents slide along level curves $\psi_{i,c}(t)=\psi_{i,0}$, where each $\psi_{i,0}$ is determined based on agent is position at t=100.35 s. In Fig. 6, actual paths of the

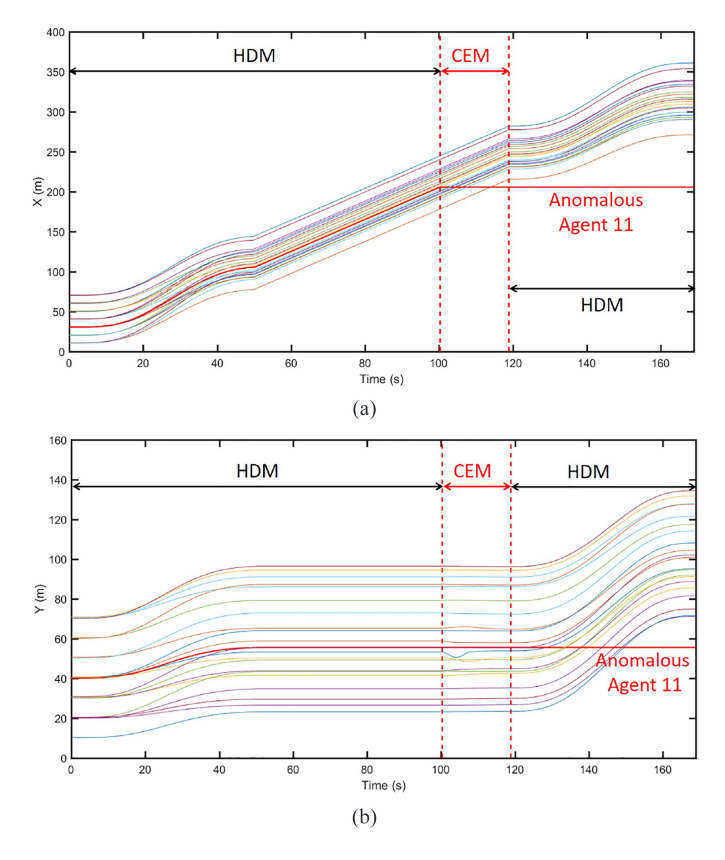


Fig. 7. (a) and (b) x and y components of actual positions of agents versus time for $t \in [0,168.91]$ s. HDM is initially active over $t \in [0,100]$ s. Agent 11 is flagged anomalous at time $t \in [100,100.35]$ s; thus, CEM is activated. At t=118.92 s, agent 11 is no longer inside the containment box $\Omega_{\rm con}$. Therefore, HDM is activated.

healthy agents, defined by $\mathcal{V}_H = \{1, \cdots, 10, 12, \cdots, 22\}$ are shown for $t \in [100.35, 118.92]$. Green markers show positions of healthy agents at t = 100.35 s when they enter CEM; black markers show positions of healthy agents at t = 118.92 s when CEM ends. Failed agent 11 is wrapped by a disk of radius 2 m centered at (205.26,55.62) in this example.

C. Motion Phase 3 (HDM)

CEM continues until switching time $118.92\,\mathrm{s}$ when failed agent 11 leaves containment box Ω_con . Fig. 4(b) shows the agents' configuration at time t=118.92. Followers use the method from Section IV to find their in-neighbors as well as communication weights. HDM remains active after t=118.92 since no other agents fail in this simulation. x and y components of actual agent positions are plotted versus time for $t\in[118.92,168.92]\,\mathrm{s}$ in Fig. 7.

VIII. CONCLUSION

This article developed a hybrid cooperative control strategy with two operational modes to manage large-scale coordination of agents in a resilient fashion. The first mode (HDM) treated agents as particles of a deformable body and is active when all agents are healthy. HDM guaranteed agents can safely initialize and coordinate their motions using the unique features

of homogeneous deformation coordination. A new CEM cooperative paradigm was proposed to handle cases in which one or more vehicles in the shared motion space fail to reach the desired coordination. In CEM, the desired vehicle coordination is treated as an ideal fluid flow and failed vehicles are excluded by closed curves. Therefore, desired trajectories for the remaining healthy vehicles can be planned, and collective motion safety for healthy vehicles can still be guaranteed with low computation overhead. To automatically initiate transition to CEM, this article contributes a strategy for quickly detecting agent failure using the unique properties of the homogeneous deformation coordination.

APPENDIX A PROOFS

Proof of Proposition 1: Given \mathbf{p}_1 , \mathbf{p}_2 , \mathbf{p}_3 , and \mathbf{p}_4^n , $\lambda_4(\mathbf{p}_1, \mathbf{p}_2, \mathbf{p}_3, \mathbf{p}_4^n, \mathbf{c}^n)$ is obtained as follows:

$$\lambda_4(\mathbf{p}_1, \mathbf{p}_2, \mathbf{p}_3, \mathbf{p}_4^n, \mathbf{c}^n) = \frac{\|\mathbf{c}^n - \mathbf{c}^2\|}{\|\mathbf{p}_4^n - \mathbf{p}_1\|}.$$
 (51)

For n=2, the nominator of (51) is 0; thus, $\lambda_4(\mathbf{p}_1, \mathbf{p}_2, \mathbf{p}_3, \mathbf{p}_4^n, \mathbf{c}^n) = 0$ for any arbitrary position of point \mathbf{c} in the motion space.

Proof of Theorem 1 [33]: If assumptions of Theorem 1 are satisfied, at least n+1 rows of matrix \mathbf{W} sum up to positive numbers that are less than 1 while the remaining rows sum up to 1. The spectral radius of $\mathbf{D} = -\mathbf{I} + \mathbf{A}$, denoted r_D , is less than 1 and eigenvalues of \mathbf{D} are all placed inside a disk of radius $r_D < 1$ centered at -1 + 0j [30]. Thus, matrix \mathbf{D} is Hurwitz. If leaders are assigned by solving (23) and (24) and followers' communication weights are obtained by solving (27), then, following properties hold: first, the communication graph \mathcal{G}_c consists at least a path directed from every leader to every follower; second, communication weights of the interior followers are all positive; third, spectral radius of matrix \mathbf{A} is less than 1 [34], and matrix $-\mathbf{I} + \mathbf{A}$ is Hurwitz. Thus, all diagonal blocks of the lower-triangular matrix $\mathbf{D} \in \mathbb{R}^{N \times N}$ are Hurwitz, which in turn implies that \mathbf{D} is Hurwitz

The reference configuration of the agents satisfy the following relation:

$$\begin{aligned} \mathbf{Y}_{0,\text{HDM}} &= \left(\mathbf{I}_{3} \otimes \mathbf{W}\right) \mathbf{Y}_{0,\text{HDM}} + \left(\mathbf{I}_{3} \otimes \mathbf{L}_{0}\right) \mathbf{Y}_{L,0,\text{HDM}} \\ \text{where } \mathbf{Y}_{L,0,\text{HDM}} &= \text{vec} \left(\begin{bmatrix} \mathbf{r}_{i_{1},0,\text{HDM}} & \cdots & \mathbf{r}_{i_{n+1},0,\text{HDM}} \end{bmatrix}^{T} \right) \in \\ \mathbb{R}^{3(n+1)\times 1}, \ \mathbf{Y}_{0,\text{HDM}} &= \text{vec} \left(\begin{bmatrix} \mathbf{r}_{i_{1},0,\text{HDM}} & \cdots & \mathbf{r}_{i_{N},0,\text{HDM}} \end{bmatrix}^{T} \right) \in \\ \mathbb{R}^{3N\times 1}, \mathbf{L}_{0} &= \begin{bmatrix} \mathbf{I}_{n+1} & \mathbf{0} \end{bmatrix}^{T} \in \mathbb{R}^{N\times (n+1)}. \text{ Therefore,} \end{aligned}$$

$$\mathbf{Y}_{0,\text{HDM}} = (\mathbf{I}_3 \otimes (\mathbf{I} - \mathbf{W})) (\mathbf{I}_3 \otimes \mathbf{L}_0) \, \mathbf{Y}_{L,0,\text{HDM}}$$
$$= (\mathbf{I}_3 \otimes (-\mathbf{D}^{-1} \mathbf{L}_0)) \, \mathbf{Y}_{L,0,\text{HDM}}. \tag{AA}$$

Because leaders form an n-D simplex and satisfy rank condition (24a), we can write

$$\mathbf{Y}_{c,\text{HDM}}(t) = (\mathbf{I}_3 \otimes \mathbf{W}_L) \, \mathbf{Y}_{L,c,\text{HDM}}(t) \tag{BB}$$

where \mathbf{W}_L is defined by (32). By equating the right-hand sides of (AA) and (BB), it is concluded that $\mathbf{W}_L = -\mathbf{D}^{-1}\mathbf{B}$. Now, we can write

$$\mathbf{Y}_d - \mathbf{Y} = (\mathbf{I}_3 \otimes \mathbf{D}) \mathbf{Y} + (\mathbf{I}_3 \otimes \mathbf{L}_0) \mathbf{Y}_{L,c,\text{HDM}}(t).$$
 (52)

On the other hand,

$$(\mathbf{I}_{3} \otimes \mathbf{D}) (\mathbf{Y} - \mathbf{Y}_{c, \text{HDM}})$$

$$= (\mathbf{I}_{3} \otimes \mathbf{D}) \mathbf{Y} - (\mathbf{I}_{3} \otimes \mathbf{D}) \left(-(\mathbf{I}_{3} \otimes \mathbf{D})^{-1} (\mathbf{I}_{3} \otimes \mathbf{L}_{0}) \mathbf{Y}_{L, c, \text{HDM}} \right)$$

$$= (\mathbf{I}_{3} \otimes \mathbf{L}) \mathbf{Y} + (\mathbf{I}_{3} \otimes \mathbf{L}_{0}) \mathbf{Y}_{L, c, \text{HDM}}$$

$$= \mathbf{Y}_{d} - \mathbf{Y}.$$
(53)

Proof of Lemma 1: While diagonal entries of matrix \mathbf{D} are all -1, off-diagonal entries of \mathbf{D} are all nonnegative. Using the Gauss–Jordan elimination method, the augmented matrix $\mathbf{D}_a = [-\mathbf{D} | \mathbf{I}] \in \mathbb{R}^{N \times 2N}$ can be converted to matrix $\tilde{\mathbf{D}}_a = [\mathbf{I} | -\mathbf{D}^{-1}] \in \mathbb{R}^{N \times 2N}$ only by performing row algebraic operations. Every entry of the lower triangle of matrix \mathbf{D} can be converted to 0 if a top row is multiplied by a positive scalar and the outcome is added to the other rows. Elements of the upper triangle of matrix $-\mathbf{D}$ can be similarly vanished, if a bottom row is multiplied by a positive scalar and the outcome is added to the other rows. Therefore, entries of matrix $-\mathbf{D}^{-1}$ are all nonnegative and \mathbf{D}^{-1} is nonpositive.

Proof of Theorem 2: Let $\mathbf{D}^{-1} = \left[\tilde{d}_{i_jh}\right] \in \mathbb{R}^{N \times N}$ where $i_j \in \mathcal{V} = \{1, \cdots, N\}$ and $h \in \{1, \cdots, N\}$. Considering (34), we can write

$$\begin{aligned} & |\mu_{i_{j},c,\text{HDM}} - \mu_{i_{j}}| \\ & = \left| -\sum_{h=1}^{N} \tilde{d}_{i_{j}h} \left(\mu_{h,d} - \mu_{h} \right) \sum_{j=1}^{n+1} B_{lj} \left(\mu_{i_{j},c} - \mu_{i_{j}} \right) \right| \\ & \leq -\sum_{j=1}^{N} D_{lj}^{-1} \left| \mu_{i_{j+n+1},c} - \mu_{i_{j+n+1}} \right| \\ & -\sum_{j=1}^{N} \tilde{d}_{i_{j}h} \hat{\Delta}_{\mu} \leq \hat{\Delta}_{\mu} \max_{i_{j} \in \mathcal{V}} \left(-\sum_{j=1}^{N} \tilde{d}_{i_{j}h} \right) = \Phi_{\max} \hat{\Delta}_{\mu} \end{aligned}$$

for $\mu \in \{x, y, z\}$. Therefore, $\|\mathbf{r}_{i_j} - \mathbf{r}_{i_j, c, \text{HDM}}\| \le \Phi_{\max} \sqrt{\hat{\Delta}_x^2 + \hat{\Delta}_y^2 + \hat{\Delta}_z^2}$ and inequality (36) is satisfied.

Proof of Theorem 3: Per the prescribed CEM protocol vehicle $i_j \in \mathcal{V}_{\mathcal{H}}$ $(j=1,\ldots,N_H)$ slides along the stream line $\psi_{i_j,c}=\psi_{i_j,0}$ at any time t. Equation (13) must be satisfied at every point $(x_{i_j,c,\mathrm{CEM}},y_{i_j,c,\mathrm{CEM}})$ and any time t. Given the sliding speed v_ϕ , the following relation holds:

$$\begin{split} &\frac{\partial \phi}{\partial x_{i_j,c,\text{CEM}}} \dot{x}_{i_j,c,\text{CEM}} + \frac{\partial \phi}{\partial y_{i_j,c,\text{CEM}}} \dot{y}_{i_j,c,\text{CEM}} = -\frac{\partial \phi}{\partial u_\infty} \dot{u}_\infty \\ &- \frac{\partial \phi}{\partial \theta_\infty} \dot{\theta}_\infty - \sum_{l=N_H+1}^N \left(\frac{\partial \phi}{\partial a_{i_l}} \dot{a}_{i_l} + \frac{\partial \phi}{\partial b_{i_l}} \dot{b}_{i_l} + \frac{\partial \phi}{\partial \Delta_{i_l}} \dot{\delta}_{i_l} \right) + v_\phi \end{split}$$

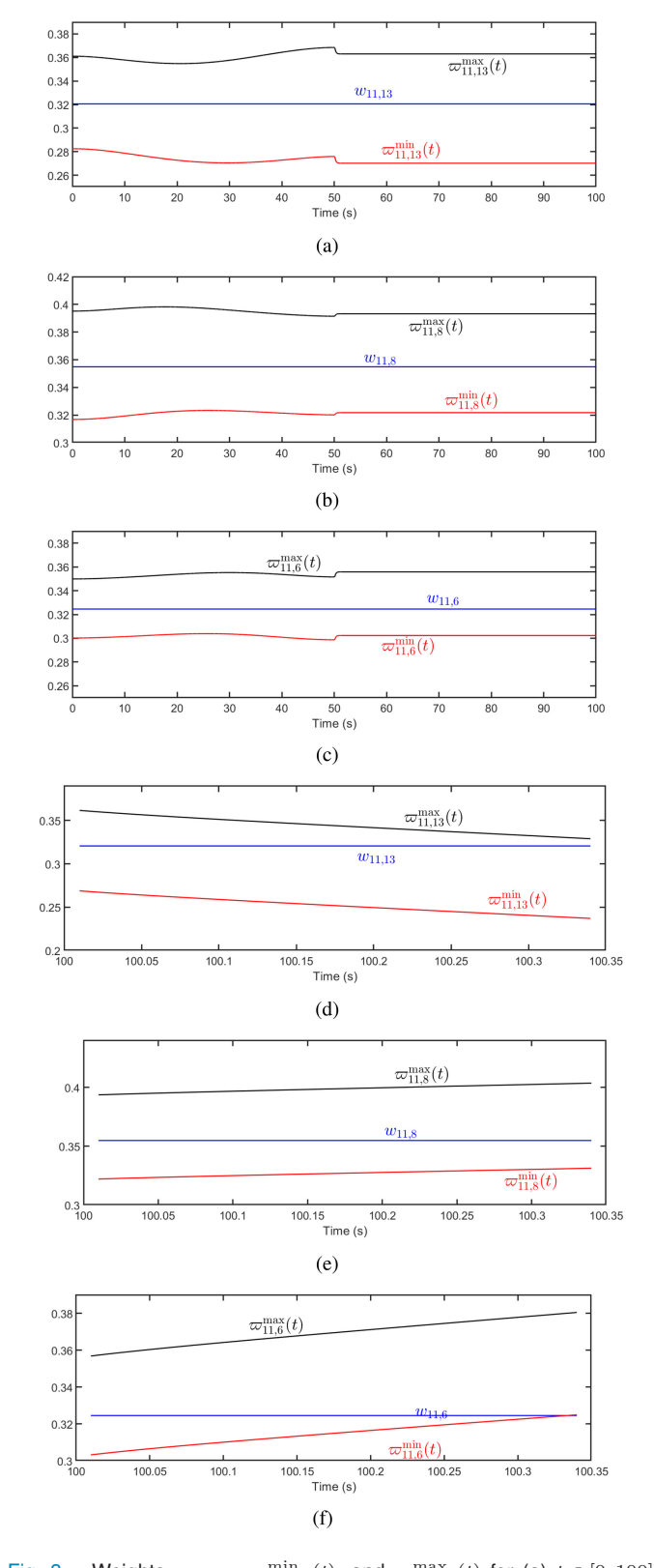


Fig. 8. Weights $w_{11,13}, \, \varpi^{\min}_{11,13}(t)$, and $\varpi^{\max}_{11,13}(t)$ for (a) $t \in [0,100]$ and (d) $t \in [100.01,100.35]$. Weights $w_{11,8}, \, \varpi^{\min}_{11,8}(t)$, and $\varpi^{\max}_{11,8}(t)$ for (b) $t \in [0,100]$ and (d) $t \in [100.01,100.35]$. Weights $w_{11,6}, \, \varpi^{\min}_{11,6}(t)$, and $\varpi^{\max}_{11,6}(t)$ for (c) $t \in [0,100]$ and (f) $t \in [100.01,100.35]$. Anomalous motion in agent 11 is detected in 0.34 s when $\varpi^{\min}_{11,6}(100.34) > w_{11,6}$.

$$j = 1, \dots, N_H, i_j \in \mathcal{V}_H, \qquad \frac{\partial \psi}{\partial x_{i_j, c, \text{CEM}}} \dot{x}_{i_j, c, \text{CEM}}$$
$$+ \frac{\partial \psi}{\partial y_{i_j, c, \text{CEM}}} \dot{y}_{i_j, c, \text{CEM}} = 0. \tag{54b}$$

Therefore, x and y components of global desired trajectory of agent $i_j \in \mathcal{V}_H$ are updated by (9), where $\mathbf{H}_{i_j,\mathrm{CEM}}$ and $\dot{\mathbf{q}}_{\mathrm{CEM}}$ are given by (43) for agent $i_j \in \mathcal{V}_H$ at any time t.

Proof of Theorem 4: If $\mathbf{r}_{i_j}(t) = \mathbf{r}_{i_j,c,\mathrm{HDM}}(t)$ for every interior follower agent $i_j \in \mathcal{V}_I(j=m_B+1,\ldots,N)$ at any time t, then $\varpi_{i_j,j_k}(t) = w_{i_j,j_k}$ $(k=1,\ldots,n+1,\ j_k \in \mathcal{N}_{i_j})$. For n=2, we define a desired triangle $j_1-j_2-j_3$ with vertices placed at $\mathbf{r}_{j_1,c,\mathrm{HDM}}$, $\mathbf{r}_{j_2,c,\mathrm{HDM}}$, and $\mathbf{r}_{j_3,c,\mathrm{HDM}}$. D_{i,j_2,j_3} denotes the distance between the global desired position of agent i_j and the triangle side j_2,j_3 , while L_{j_1,j_2,j_3} denotes the distance between the desired position of agent j_1 and the side j_2-j_3 of the desired triangle. We also define an "actual" triangle with vertices positioned at \mathbf{r}_{j_1} , \mathbf{r}_{j_2} , and \mathbf{r}_{j_3} . When $\|\mathbf{r}_{i_j}(t)-\mathbf{r}_{i_j,c,\mathrm{HDM}}(t)\|\leq \Delta$ is satisfied for agent $i_j\in\mathcal{V}$ at any time t, we have

$$d_{i_j,j_2,j_3}(t) - 2\Delta \le D_{i_j,j_2,j_3}(t) \le d_{i_j,j_2,j_3}(t) + 2\Delta \quad (55a)$$

$$l_{j_1,j_2,j_3}(t) - 2\Delta \le L_{j_1,j_2,j_3}(t) \le l_{j_1,j_2,j_3}(t) + 2\Delta. \quad (55b)$$

Therefore, $w_{i_j,j_1} = \frac{D_{i_j,j_2,j_3}(t)}{L_{j_1,j_2,j_3}(t)} \in [\frac{d_{i_j,j_2,j_3}(t)-2\Delta}{l_{j_1,j_2,j_3}(t)+2\Delta}, \frac{d_{i_j,j_2,j_3}(t)+2\Delta}{l_{j_1,j_2,j_3}(t)-2\Delta}]$ (See Fig. 3(b)). For n=3, vertices of the desired tetrahedron $j_1-j_2-j_3-j_4$ are placed at $\mathbf{r}_{j_1,c,\mathrm{HDM}}, \mathbf{r}_{j_2,c,\mathrm{HDM}}, \mathbf{r}_{j_3,c,\mathrm{HDM}},$ and $\mathbf{r}_{j_4,c,\mathrm{HDM}}$; vertices of the "actual" tetrahedron are positioned at $\mathbf{r}_{j_1}, \mathbf{r}_{j_2}, \mathbf{r}_{j_3}$, and \mathbf{r}_{j_3} . D_{i_j,j_1,j_2,j_3} denotes the distance between the global desired position of agent i_j and the tetrahedron surface j_2, j_3, j_4 . L_{j_1,j_2,j_3,j_4} denotes the distance between the desired position of agent j_1 and the surface $j_2-j_3-j_4$ of the desired tetrahedron. Assuming every agent $i_j \in \mathcal{V}$ satisfies safety constraint (36),

$$d_{i_j,j_2,j_3,j_4}(t) - 2\Delta \le D_{i_j,j_2,j_3,j_4}(t) \le d_{i_j,j_2,j_3,j_4}(t) + 2\Delta$$
(56a)

$$l_{j_1,j_2,j_3,j_4}(t) - 2\Delta \le L_{j_1,j_2,j_3,j_4}(t) \le l_{j_1,j_2,j_3,j_4}(t) + 2\Delta$$
(56b)

Therefore.

$$\begin{split} w_{i_j,j_1} &= \frac{D_{i_j,j_2,j_3,j_4}(t)}{L_{j_1,j_2,j_3,j_4}(t)} \\ &\in \left[\frac{d_{i_j,j_2,j_3,j_4}(t) - 2\Delta}{l_{j_1,j_2,j_3,j_4}(t) + 2\Delta}, \frac{d_{i_j,j_2,j_3,j_4}(t) + 2\Delta}{l_{j_1,j_2,j_3,j_4}(t) - 2\Delta}\right]. \end{split}$$

APPENDIX B

Assignment of Proximity Graph at Time t=0

This section explains how agents are classified as boundary agents, interior agents, leaders, and followers given the initial reference configuration shown in Fig. 4(a). The agent team consists of 22 agents ($\mathcal{V} = \{1, \dots, 22\}$). Set $\mathcal{V}_B = \{i_1, \dots, i_{10}\}$ defines the boundary agents, where $i_1 = 1$, $i_2 = 10$, $i_3 = 22$, $i_4 = 2$, $i_5 = 3$, $i_6 = 12$, $i_7 = 14$, $i_8 = 18$, $i_9 = 20$, $i_{10} = 21$.

While $\mathcal{V}_L = \{i_1, i_2, i_3\}$ specifies the leaders, $\mathcal{V}_B \subset \mathcal{V}_L$ defines the boundary followers. Boundary followers all communicate with leaders i_1, i_2 , and i_3 . Note that links from leaders i_1, i_2 , and i_3 to boundary followers are not shown in Fig. 4. Additionally, $\mathcal{V}_I = \{i_{11}, \ldots, i_{22}\}$ defines interior agents, where $i_{11} = 4, i_{12} = 5, i_{13} = 6, i_{14} = 7, i_{15} = 8, i_{16} = 9, i_{17} = 11, i_{18} = 13, i_{19} = 15, i_{20} = 16, i_{21} = 17,$ and $i_{22} = 19$ are the interior agents. Note that $\mathcal{V}_I \subset \mathcal{V}_F$ are all followers.

APPENDIX C ANOMALY DETECTION EXAMPLE

In Fig. 8, reference communication weights $w_{11,13}, w_{11,18}$, and $w_{11,6}$ and transient communication weights $\varpi_{11,13}^{\min}(t)$, $\varpi_{11,13}^{\max}(t), \ \varpi_{11,18}^{\min}(t), \ \varpi_{11,18}^{\min}(t), \ \varpi_{11,6}^{\min}(t), \ \text{and} \ \varpi_{11,6}^{\min}(t)$ are plotted versus time t for $t \in [0,100]$ and $t \in [100.01,100.35]$, where interagent communication is defined by the graph shown in Fig. 4(a). As shown in Fig. 8(a)–(c), conditions $\varpi_{11,13}^{\min}(t) \leq w_{11,13} \leq \varpi_{11,13}^{\max}(t), \ \varpi_{11,8}^{\min}(t) \leq w_{11,8} \leq \varpi_{11,8}^{\max}(t), \ \text{and} \ \varpi_{11,6}^{\min}(t) \leq w_{11,6} \leq \varpi_{11,6}^{\min}(t) \otimes w_{11,6} \otimes w_{11$

REFERENCES

- F. Xiao, L. Wang, J. Chen, and Y. Gao, "Finite-time formation control for multi-agent systems," *Automatica*, vol. 45, no. 11, pp. 2605–2611, 2009.
- [2] M. Wiering, "Multi-agent reinforcement learning for traffic light control," in *Proc. 17th Int. Conf. Mach. Learn.*, 2000, pp. 1151–1158.
- [3] Z. Li, F. R. Yu, and M. Huang, "A distributed consensus-based cooperative spectrum-sensing scheme in cognitive radios," *IEEE Trans. Veh. Technol.*, vol. 59, no. 1, pp. 383–393, Jan. 2010.
- [4] J. Wu, S. Yuan, S. Ji, G. Zhou, Y. Wang, and Z. Wang, "Multi-agent system design and evaluation for collaborative wireless sensor network in large structure health monitoring," *Expert Syst. Appl.*, vol. 37, no. 3, pp. 2028–2036, 2010.
- [5] W. Ren and R. Beard, "Decentralized scheme for spacecraft formation flying via the virtual structure approach," *J. Guid., Control, Dyn.*, vol. 27, no. 1, pp. 73–82, 2004.
- [6] W. Ren and R. Beard, "Virtual structure based spacecraft formation control with formation feedback," in *Proc. AIAA Guid.*, *Navigation, Control Conf. Exhib.*, 2002, p. 4963.
- [7] W. Hou, M. Fu, H. Zhang, and Z. Wu, "Consensus conditions for general second-order multi-agent systems with communication delay," *Automatica*, vol. 75, pp. 293–298, 2017.
- [8] J. M. Kim, J. B. Park, and Y. H. Choi, "Leaderless and leader-following consensus for heterogeneous multi-agent systems with random link failures," *IET Control Theory Appl.*, vol. 8, no. 1, pp. 51–60, 2014.
- [9] M. Defoort, A. Polyakov, G. Demesure, M. Djemai, and K. Veluvolu, "Leader-follower fixed-time consensus for multi-agent systems with unknown non-linear inherent dynamics," *IET Control Theory Appl.*, vol. 9, no. 14, pp. 2165–2170, 2015.
- [10] Z. Zuo and L. Tie, "Distributed robust finite-time nonlinear consensus protocols for multi-agent systems," *Int. J. Syst. Sci.*, vol. 47, no. 6, pp. 1366–1375, 2016.
- [11] X. Lin and Y. Zheng, "Finite-time consensus of switched multiagent systems," *IEEE Trans. Syst., Man, Cybern., Syst.*, vol. 47, no. 7, pp. 1535–1545, Jul. 2017.
- [12] H. Su, Y. Ye, Y. Qiu, Y. Cao, and M. Z. Chen, "Semi-global output consensus for discrete-time switching networked systems subject to input saturation and external disturbances," *IEEE Trans. Cybern.*, vol. 49, no. 11, pp. 3934–3945, Nov. 2019.
- [13] C.-L. Liu and F. Liu, "Stationary consensus of heterogeneous multi-agent systems with bounded communication delays," *Automatica*, vol. 47, no. 9, pp. 2130–2133, 2011.

- [14] A. Papachristodoulou, A. Jadbabaie, and U. Munz, "Effects of delay in multi-agent consensus and oscillator synchronization," *IEEE Trans. Autom. Control*, vol. 55, no. 6, pp. 1471–1477, Jun. 2010.
- [15] R. Cepeda-Gomez and N. Olgac, "Exhaustive stability analysis in a consensus system with time delay and irregular topologies," *Int. J. Control*, vol. 84, no. 4, pp. 746–757, 2011.
- [16] H. J. LeBlanc, Resilient Cooperative Control of Networked Multi-Agent Systems. Nashville, TN, USA: Vanderbilt University, 2012.
- [17] Y. Shang, "Resilient consensus of switched multi-agent systems," Syst. Control Lett., vol. 122, pp. 12–18, 2018.
- [18] S. M. Dibaji and H. Ishii, "Resilient consensus of second-order agent networks: Asynchronous update rules with delays," *Automatica*, vol. 81, pp. 123–132, 2017.
- [19] H. J. LeBlanc, H. Zhang, X. Koutsoukos, and S. Sundaram, "Resilient asymptotic consensus in robust networks," *IEEE J. Sel. Areas Commun.*, vol. 31, no. 4, pp. 766–781, Apr. 2013.
- [20] H. Liu, G. Xie, and L. Wang, "Necessary and sufficient conditions for containment control of networked multi-agent systems," *Automatica*, vol. 48, no. 7, pp. 1415–1422, 2012.
- [21] M. Ji, G. Ferrari-Trecate, M. Egerstedt, and A. Buffa, "Containment control in mobile networks," *IEEE Trans. Autom. Control*, vol. 53, no. 8, pp. 1972–1975, Sep. 2008.
- [22] T.-H. Cheng, Z. Kan, J. R. Klotz, J. M. Shea, and W. E. Dixon, "Event-triggered control of multiagent systems for fixed and time-varying network topologies," *IEEE Trans. Autom. Control*, vol. 62, no. 10, pp. 5365–5371, Oct. 2017.
- [23] W. Li, L. Xie, and J.-F. Zhang, "Containment control of leader-following multi-agent systems with Markovian switching network topologies and measurement noises," *Automatica*, vol. 51, pp. 263–267, 2015.
- [24] X. Wang, S. Li, and P. Shi, "Distributed finite-time containment control for double-integrator multiagent systems," *IEEE Trans. Cybern.*, vol. 44, no. 9, pp. 1518–1528, Sep. 2014.
- [25] Y. Zhao, Z. Duan, G. Wen, and Y. Zhang, "Distributed finite-time tracking control for multi-agent systems: An observer-based approach," Syst. Control Lett., vol. 62, no. 1, pp. 22–28, 2013.
- [26] J. Shen and J. Lam, "Containment control of multi-agent systems with unbounded communication delays," *Int. J. Syst. Sci.*, vol. 47, no. 9, pp. 2048–2057, 2016.
- [27] Q. Xiong, P. Lin, W. Ren, C. Yang, and W. Gui, "Containment control for discrete-time multiagent systems with communication delays and switching topologies," *IEEE Trans. Cybern.*, vol. 49, no. 10, pp. 3827–3830, Oct 2019
- [28] S. Zhao, "Affine formation maneuver control of multiagent systems," *IEEE Trans. Autom. Control*, vol. 63, no. 12, pp. 4140–4155, Dec. 2018.

- [29] Y. Xu, S. Zhao, D. Luo, and Y. You, "Affine formation maneuver control of multi-agent systems with directed interaction graphs," in *Proc. IEEE* 37th Chin. Control Conf., 2018, pp. 4563–4568.
- [30] H. Rastgoftar, Continuum Deformation of Multi-Agent Systems. New York, NY, USA: Springer, 2016.
- [31] H. Rastgoftar and S. Jayasuriya, "Evolution of multi-agent systems as continua," J. Dyn. Syst., Meas., Control, vol. 136, no. 4, 2014, Art. no. 041014
- [32] H. Rastgoftar, J.-B. Jeannin, and E. Atkins, "Formal specification of continuum deformation coordination," in *Proc. IEEE Amer. Control Conf.*, 2019, pp. 3358–3363.
- [33] H. Rastgoftar, "Safe affine transformation of a large-scalemulti-quadcopter system (MQS)," Special Issue IEEE Trans. Control Netw. Syst., to be published.
- [34] H. Rastgoftar, E. M. Atkins, and D. Panagou, "Safe multiquadcopter system continuum deformation over moving frames," *IEEE Trans. Control Netw. Syst.*, vol. 6, no. 2, pp. 737–749, Jun. 2019.



Hossein Rastgoftar (Member, IEEE) received the B.Sc. degree in mechanical engineering-thermo-fluids from Shiraz University, Shiraz, Iran, the M.S. degrees in mechanical systems and solid mechanics from Shiraz University and the University of Central Florida, Orlando, FL, USA, and the Ph.D. degree in mechanical engineering from Drexel University, Philadelphia, PA, USA, in 2015.

He currently an Assistant Professor with Villanova University, Philadelphia, PA, USA and an

Adjunct Assistant Professor with the University of Michigan, Ann Arbor, MI, USA. He was an Assistant Research Scientist at the Aerospace Engineering Department from 2017 to 2020. Prior to that he was a Post-doctoral Researcher at the University of Michigan from 2015 to 2017. His current research interests include dynamics and control, multiagent systems, cyberphysical systems, and optimization and Markov decision processes.